DESIGN AND ELECTRONIC COMPENSATION OF A DIAMAGNETIC LOOP AND ITS APPLICATION IN THE ASDEX TOKAMAK

J. Gernhardt, F. Schneider

Februar 1986

IPP III/84

MAX-PLANCK-INSTITUT FÜR PLASMAPHYSIK

8046 GARCHING BEI MÜNCHEN

MAX-PLANCK-INSTITUT FÜR PLASMAPHYSIK

GARCHING BEI MÜNCHEN

DESIGN AND ELECTRONIC COMPENSATION OF A DIAMAGNETIC LOOP AND ITS APPLICATION IN THE ASDEX TOKAMAK

J. Gernhardt, F. Schneider

IPP III/84

Februar 1986

Die nachstehende Arbeit wurde im Rahmen des Vertrages zwischen dem Max-Planck-Institut für Plasmaphysik und der Europäischen Atomgemeinschaft über die Zusammenarbeit auf dem Gebiete der Plasmaphysik durchgeführt.

TABLE OF CONTENTS

IPP III/84

J. Gernhardt
F. Schneider

DESIGN AND ELECTRONIC COMPENSATION OF A DIAMGANETIC LOOP AND ITS APPLICATION IN THE ASDEX TOKAMAK

February 1986

ABSTRACT

Owing to the perpendicular motion of electrons and ions the plasma excludes a small amount $\delta\Phi$ of the toroidal flux Φ. Measuring $\delta\Phi$ allows determination of the diamagnetic beta poloidal $\beta_{p\perp}$, defined as the ratio of transverse plasma pressure to magnetic pressure at the plasma surface. $\beta_{p\perp}$ is measured by a separate loop mounted outside of the stainless-steel vacuum vessel. The design and mounting of the loop are described. As in tokamaks one has $\delta\Phi/\Phi \sim 10^{-4}$, even very slight magnetic stray fields, coil displacements and eddy currents in the structure during the discharge pulse can influence the diamagnetic signal. We show the separate interference of vertical, ohmic-heating, divertor, radial and toroidal fields, and finally the effect of misalignment with respect to the plasma current. We also describe the method and the electric system for compensating these spurious effects. The final section presents experimental results which demonstrate the operation of the diamagnetic loop during the ohmic-heating and neutral-injection phases.

1. INTRODUCTION

The potential of the diamagnetic effect of a tokamak plasma as a means of measuring the transverse plasma energy $n \cdot k \cdot [T_e + T_i]$ (symbol definitions and their units are shown in the Appendix) has long been known /1/. It provides a continuous measure of the transverse plasma energy, time-dependent througout a single discharge, without requiring a knowledge of the radial profiles of T_e, T_i, n_e and n_i. But as the excluded toroidal flux ($\delta\Phi$) is extremely small ($\delta\Phi/\Phi \sim 10^{-4}$), this diagnostic technique has been hampered by its low accuracy in conjunction with the low plasma energy content of the small tokamak machines of the past.

As $\delta\Phi$ increases as the square of the plasma current, the use of the diamagnetic effect has gained new importance. In future devices the diamagnetic signal will probably be one of the more important diagnostic

methods able to give information on the internal energy content of the plasma, when other diagnostic techniques may be subject to increasing limitations.
But it must still be able to detect a signal change of the order of 0.1 mT in the presence of a toroidal magnetic field of 2 to 3 T in the hostile environment of a tokamak discharge.

In this paper the technical realisation for diamagnetic measurements in the ASDEX Tokamak are described and experimental examples are given. ASDEX is a large divertor Tokamak with major radius R_o = 165 cm and minor radius a = 40 cm. ASDEX is operated between $B_{\phi,TF(0)}$ = 1.2 and 2.7 T and a plasma current between 170 and 450 kA. The ASDEX Tokamak is described in Ref. /2/.

For future plasma devices we would recommend for the purpose of redundance that at least two separate diamagnetic loops be mounted at different toroidal positions to increase the reliability of this diagnostic technique.

2. THEORY

2.1 Measurement of poloidal beta by the diamagnetic effect

In a Tokamak configuration (see Fig. 1) the plasma is kept in equilibrium by poloidal magnetic fields. When the kinetic plasma pressure remains smaller than the poloidal magnetic pressure at the plasma boundary (r = a), $\beta_{p\perp}$ is smaller than one and the difference is compensated by a decrease of the toroidal magnetic field within the plasma.
Beta poloidal $\beta_{p\perp}$ is defined as the ratio of the kinetic plasma pressure <p> (acting perpendicularly to B_θ towards the plasma centre) to the poloidal magnetic pressure $B_\theta^2/2\,\mu_o$ at the plasma boundary (ρ = r/a = 1):

$$\beta_{p\perp} = \frac{<p>}{\frac{B_\theta^2(1)}{2\mu_o}} \qquad (1)$$

$$<p> = \frac{1}{\pi a^2} \int_{r=o}^{r=a} k\,[n_e(r) \cdot T_e(r) + n_i(r) \cdot T_i(r)] \cdot 2\pi\, r \cdot dr \qquad (2)$$

The total (toroidal) beta ß is defined as the ratio of the kinetic plasma pressure <p> to the total magnetic pressure ($B_\theta^2/2\mu_o + B_\phi{}^2/2\mu_o$), where B_θ is the poloidal magnetic field at the plasma boundary ($\rho = 1$) and B_ϕ the toroidal magnetic field taken from the plasma centre ($\rho = 0$; R_o):

$$ß = \frac{<P>}{\frac{1}{2\mu_o}\,[B_\theta^2(1)+B_\phi^2\,(0)]} \tag{3}$$

In tokamaks $B_\theta \ll B_\phi$ we therefore have:

$$ß = \frac{<P>}{\frac{B_\phi^2\,(0)}{2\mu_o}} \tag{4}$$

Toroidal beta ß and poloidal beta $ß_{p\perp}$ are related as follows:

$$ß_t = ß = \frac{ß_{p\perp}}{q^2 \cdot A^2} \tag{5}$$

A is the aspect ratio $A = R_o/a$ and q the safety factor:

$$q = \frac{2\pi}{\mu_o} \cdot \frac{a^2}{R_o} \cdot \frac{B_\phi\,(0)}{J_p} \tag{6}$$

If the plasma current J_p is known, then equation (1) can be rewritten as

$$\oint B_\theta \cdot dl = \mu_o \cdot J_p \tag{7}$$

$$B_\theta(1) = \frac{\mu_o \cdot J_p}{2\pi\, a} \tag{8}$$

$$ß_{p\perp} = \frac{8 \cdot \pi^2}{\mu_o} \cdot \frac{a^2}{J_p^2}\ <P> \tag{9}$$

The pressure-balance equation, when the curvature of the torus is neglected, can be written in the form

$$<P> = \frac{1}{2 \cdot \mu_o}\,[B_\theta^2(1) - (<B_\phi^2> - B_{\phi\,,TF(0)}^2)] \tag{10}$$

$B_{\phi\,,TF(0)}$ is the longitudinal magnetic field at the plasma centre, is produced by just the toroidal field coils. B_ϕ, the total longitudinal magnetic field inside the plasma column, is produced by the toroidal

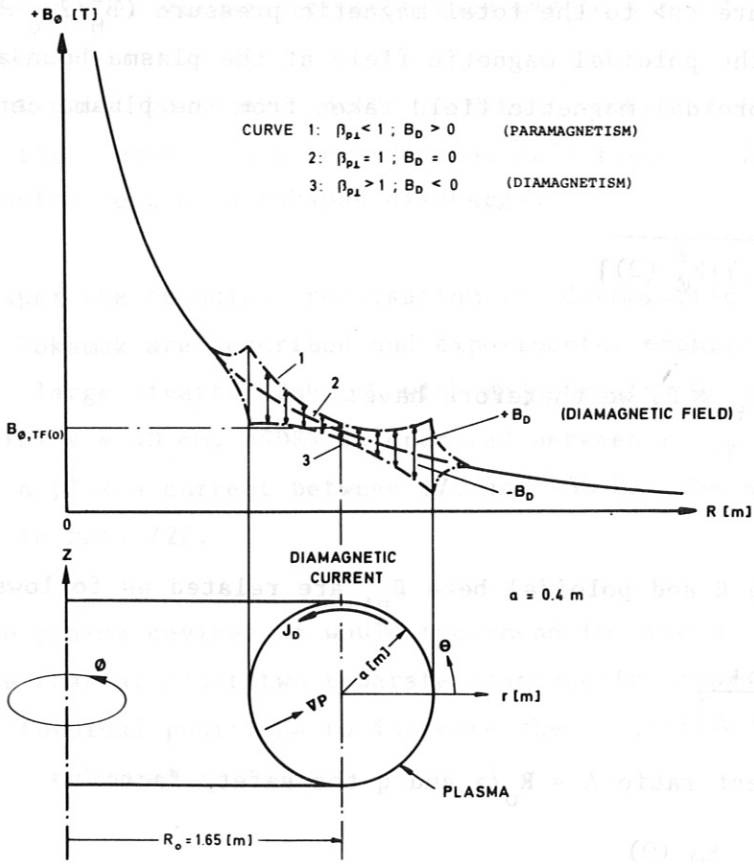

SKETCH 1

field coils and the diamagnetic currents at the plasma surface. The angle brackets denote averaging over the whole plasma column cross-section. For a given plasma current J_p and kinetic plasma pressure <p>, the difference $\langle B_\phi^2 \rangle - B_{\phi,TF(0)}^2$ is adjusted in such a way that the pressure-balance equation is satisfied. In tokamaks $B_\phi \gg B_\theta$ the relative magnitude of diamagnetism (or paramagnetism) is therefore small and can be represented as

$$\delta\phi = \pi a^2 \left(\langle B_\phi - B_{\phi,TF(0)} \rangle\right) \qquad (11)$$

$\delta\phi$ is the diamagnetic flux of the longitudinal magnetic field in the plasma column. Substituting this expression in the pressure-balance equation, we obtain

$$\beta_{p\perp} = 1 - 2 \frac{B_{\phi,TF(0)}}{B_\theta^2(1)} \cdot \frac{\delta\phi}{\pi a^2} \qquad (12)$$

where $\delta\Phi = U_D \cdot \frac{U_D'}{N_1}$ (13)

With equation (8) we get

$$\beta_{p\perp} = 1 - 8\pi \cdot \frac{B_{\Phi,TF(0)}}{(\mu_o \cdot J_p)^2} \cdot \delta\Phi \qquad (14)$$

N_1 is the number of windings of the diamagnetic loop

$\beta_{p\perp} < 1$ yields $\delta\Phi > 0$ (paramagnetism)

$\beta_{p\perp} = 1$ yields $\delta\Phi = 0$

$\beta_{p\perp} > 1$ yields $\delta\Phi < 0$ (diamagnetism)

If $\beta_{p\perp} \ll R_o/a$, then the corrections for the torus curvature are not significant. If a plasma has a horizontal displacement Δ_H relative to the major radius R_o, then the difference $(\beta_{p\perp}-1)$ has to be corrected with the relative error Δ_H/R_o, i.e. the value of $B_{\Phi,TF(0)}$ in equation (14) should be that at the displaced plasma centre. $\beta_{p\perp}$ in equation (14) is derived from the experimentally measured quantities J_p, $\delta\Phi$ and $B_{\Phi,TF(0)}$.

The plasma current J_p can be measured with a Rogowski coil wound around the vacuum vessel. The induced voltage in the Rogowski coil is integrated with an active integrator. The output signal of the integrator is proportional to the plasma current.

$B_{\Phi,TF(0)}$ is measured with a coil located inside the toroidal field windings. The induced voltage of the coil is integrated and is proportional to the toroidal magnetic field.

The diamagnetic flux change $\delta\Phi$ can be measured by integrating the transient voltage U_D' induced in the diamagnetic loop wound around the minor circumference of the plasma. To measure the diamagnetic flux change $\delta\Phi$, two sets of windings are used. The first set of windings (number of windings, N1) encircles the whole plasma area and measures the total toroidal flux $\Phi = \delta\Phi + \Phi_{TF}$ created by the diamagnetic current of the plasma and the toroidal field coils. A second set of compensation windings (number of winding, N_2) which encircles the outer periphery of the vacuum vessel measures the toroidal flux Φ_{TF} created by the toroidal field coils alone (see Fig. 2). The flux differences are given by

$$\delta\Phi = \Phi - \Phi_{TF} \qquad (15)$$

The numbers of windings of the two coils are chosen such that when there is no plasma the flux difference $\delta\Phi$ is zero:

$$N_1 \cdot \Phi = N_2 \cdot \Phi_{TF,COM} \tag{16}$$

$$\text{i.e. } N_1 \cdot A_D \cdot B_{\Phi,TF(0)} = N_2 \cdot A_{com} \cdot B_{\Phi,TF(0)} \tag{17}$$

with $\delta\Phi \ll \Phi_{TF}$ and $\Phi = \int B \cdot dA$ (A = loop area) it follows that

$$\frac{N_1}{N_2} = \frac{A_{com}}{A_D} \tag{18}$$

The sketches 2 and 3 show the areas which are encircled by the diamagnetic loops and the compensation loops on ASDEX.

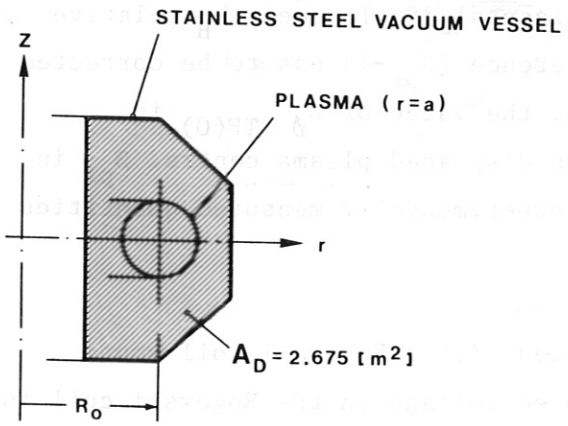

SKETCH 2

flux area measured with diamagnetic loop (N_1)

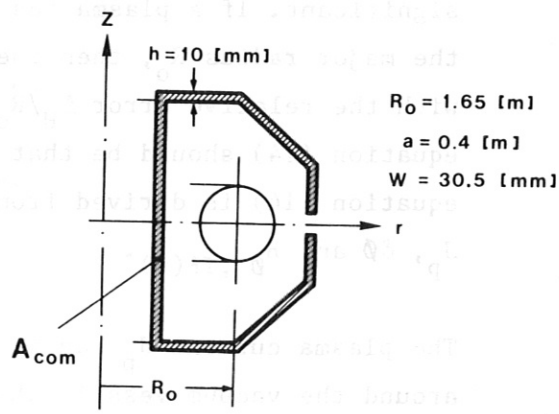

SKETCH 3

flux area measured with compensating loop (N_2)

2.2 Discussion of equation (19) below

Equation (14) solved for $\delta\Phi$ gives

$$\delta\Phi = \frac{(\mu_o \cdot J_p)^2}{8\pi \cdot B_{\Phi,TF(0)}} (1-\beta_{p_\perp}) = \frac{1}{N_1} \int_0^t U'_D \cdot dt \quad [Vs] \tag{19}$$

2.2.1 During the plasma start-up T_e, T_i and n are very small and $\beta_{p_\perp} \sim 0$. The diamagnetic coil signal $\delta\Phi$ therefore only depends on J_p^2.

($B_{\emptyset,TF(0)}$ is constant during the time of the plasma current).

2.2.2 If $\beta_{p\perp} = 1$, for example during neutral injection, the diamagnetic flux signal $\delta\emptyset$ is zero.

2.2.3 With $\beta_{p\perp} > 1$, for example during high-power neutral injection into a discharge with good confinement (H-mode discharge /3/), the diamagnetic flux signal $\delta\emptyset$ will be negative.

2.3 Discussion of equation (14)

If $\beta_{p\perp}$ is very small, for example during suprathermal plasma discharges /4/ with $\beta_{p\perp} = 0.1$, then an inaccuracy of 10 % in $\delta\emptyset$ will create an error of several 100 % in $\beta_{p\perp}$.

2.4 Numerical relations of the diamagnetic loop signals in ASDEX

If we assume plasma profiles in ASDEX of the form

$$T_e = T_{eo}\,(1-\rho^2)^{\alpha}$$
$$T_i = T_{io}\,(1-\rho^2)^{\alpha}$$
$$n_e = n_{eo}\,(1-\rho^2)^{\gamma}$$
$$n = n_i = n_e$$

then equation (2) yields

$$\langle P\rangle = \frac{n_{eo}\,(T_{eo} + T_{io})}{\alpha + \gamma + 1} \cdot k \qquad (20)$$

Equation (9) and (20) give

$$\beta_{p\perp} = \frac{8 \cdot \pi^2 \cdot a^2}{\mu_o \cdot J_p^{\,2}} \cdot k' \cdot \frac{n_{eo}\,(T_{eo}+T_{io})}{\alpha + \gamma + 1} \qquad (21)$$

Inserting equation (21) in equation (19) gives

$$\delta\emptyset = \frac{U_D \cdot \tau}{N_1} = \frac{(\mu_o \cdot J_p)^2}{8 \cdot \pi \cdot B_{\emptyset,TF(0)}} - \mu_o \cdot \pi \, \frac{a^2}{B_{\emptyset,TF(0)}} \cdot k' \cdot n_{eo} \frac{(T_{eo}+T_{io})}{\alpha + \gamma + 1} \qquad (22)$$

Figure 3 shows equations (14), (21) and (22) with the following parameters:

J_p = 300, 400 and 500 [kA]

$B_{\emptyset,TF(0)}$ = 2,2 [T]

$a = 0{,}4$ [m]

$n_{eo} = 6{,}55 \cdot 10^{19}$ [m^{-3}]

$\alpha = 2$

$\gamma = 1$

$N_1 = 2$ windings

$\tau = 2$ [ms]

The chart in Fig. 3 can be used as a quick reference to find β_{p1} and estimate the plasma temperatures ($T_{eo}+T_{io}$) at the plasma centre when the integrated voltage (active integrator with $\tau = 2$ ms) of the diamagnetic loop ($N_1 = 2$ windings) is known.

3. DESIGN OF THE DIAMAGNETIC LOOP FOR ASDEX

On the ASDEX experiment we use a compensated diamagnetic loop consisting of a main loop, two turns ($N_1 = 2$, see item 1 in Fig. 4) for measuring the total toroidal flux $\emptyset$, and a compensating, multiturn loop ($N_2 = 37$, see items 2 to 9 in Fig. 4) for measuring only the toroidal flux of the toroidal field coils $\emptyset_{TF}$. Both are wound on a common support encircling the vacuum vessel minor circumference. The 37 windings are made out of Kapton-insulated copper wire (AWG 26; $A_{Cu} = 0{,}141$ mm^2) with an outside diameter of 0.81 mm, around a 10 mm (h) thick and 30.5 mm (w) wide sheet of silicon resin glass fibre. Eight of those sections are assembled poloidally around the stainless-steel vacuum vessel (see Fig. 5 to 8). This set of coils, the active area of which encircles, but does not contain the plasma cross-section, are electrically connected in series inside the control room. The two turns of the diamagnetic loop and the 8 sections of compensation loop have to be aligned parallel to the poloidal magnetic field to eliminate all spurious voltages induced by the poloidal magnetic field variation.

During the vacuum vessel assembly, the diamagnetic and compensation coils were mounted on the outside of the vacuum vessel, aligned with a precision electronic water level (accuracy: 0.01 mm per metre length) and mounted on several micrometer screw adjustments (see Fig. 9) between the vacuum vessel and the coil frame.

During this mounting period the poloidal magnetic field axis was unknown and therefore the axis of the vacuum vessel itself was used for the alignment.

Because of the discrepancy between the poloidal magnetic field axis and the vacuum vessel axis there is an induced stray signal $\delta\phi_s$ created by the magnetic field from all poloidal field windings and the magnetic field change of the plasma current; this stray signal $\delta\phi_s$ is about 10 % of the value of $\delta\phi$, for a normal plasma current discharge of $J_p \sim 300$ kA; $n_e \sim 3 \cdot 10^{13}$ cm^{-3} and $\beta_{p\perp}$ of about 0.3.
A stray field of $\delta\phi_s = 0.1 \cdot \delta\phi$ would add an error of $\Delta\beta_{p\perp} = 0.07$ to the measured $\beta_{p\perp} \sim 0.3$ (see Sec. 5).

We also mounted an additional compensating loop on the vacuum vessel to eliminate the radial movement of the vessel during the plasma shots /5/. So far this coil arrangement has not been used because the radial movement of the vacuum vessel is <0.1 mm. This displacement induces only a small change in $\delta\phi$ during the flat-top phase of the toroidal field and the correction is done by the computer program (see Sec. 8.9).

4. ELECTRICAL NOISE (PICK-UP)

During an ohmic plasma discharge with

$J_p \sim 300$ kA
$n_e \sim 3 \cdot 10^{13}$ cm^{-3}
$\beta_{p\perp} \sim 0{,}3$

the total voltage U_D' induced in the compensated diamagnetic loop is about 10 mV. Because of this low magnitude, care has to be taken that this signal is not disturbed by other galvanic, magnetic or capacitive effects (Electro magnetic interference EMI; /6/, /7/).

4.1 Influence of eddy currents on the diamagnetic signal

During the rising and decaying phase of the toroidal magnetic field, a complete compensation of the diamagnetic loop and compensation loop is not possible because of eddy currents in the vacuum vessel and the geometric differences of the two coil systems. The diamagnetic

measurement therefore only takes place during the flat-top phase of the toroidal magnetic field. In ASDEX the flat-top time is at least 5 sec. It reduces the error if the toroidal field is already constant several 100 msec before and after the plasma current pulse so that the right zero balance of the diamagnetic signal (see Fig. 10) can be measured shortly before and after the plasma current occurs.

4.2 Current leads to the poloidal and toroidal coils may disturb the diamagnetic signal. The diamagnetic loop and the compensation loop are toroidally located as far away as possible from these current leads (see Fig. 11), so as to be as free of stray fields as possible.

4.3 Mechanical vibrations

The diamagnetic measurement is also very sensitive to mechanical vibrations during the discharge so that the loops must be installed on a rigid support structure. All mechanical vibrations are avoided near the diamagnetic loop. For example, no vacuum pumps are located close to the diamagnetic loop.

4.4 Displacements

The diamagnetic loop is mounted on the vacuum vessel made of stainless steel 20 and 30 mm thick at a position where almost no displacement during the plasma shot takes place. A radially inward displacement of the outer vessel wall of less than 0.1 mm is measured.

4.5 Insulation gaps of the vacuum vessel

The diamagnetic loop should not be placed near the insulation gap of a vacuum vessel because currents flow along the insulation gap in the poloidal direction, creating toroidal magnetic stray fields.

4.6 Electromagnetic shielding

The diamagnetic loop has to be electromagnetically shielded to reduce the common mode voltage as far as possible for the electronic circuitry. In Fig. 6, a copper shield 0.5 mm thick with a 0.8 mm wide slit every 200 mm is shown. In the lower part of the pictures the diamagnetic compensation coil system is shown covered with the copper shielding, with a Teflon foil glued to the top of it to avoid ground loops. The upper part of the picture shows two compensation coil systems with the 37 windings. Each of the eight poloidally mounted copper shields of the compensation coils is connected to the stainless-

steel vacuum vessel only at one point to prevent ground loops.

4.7 Thermo-voltage

The thermo-voltage created in the electrical circuit of the diamagnetic loop system by soldering different materials together has to be avoided as far as possible. A specially designed active integrator described in Sec. 6 with an automatic offset control (up to 1 mV) can handle this thermo-voltage.

4.8 Reduction of magnetic interference by twisted cables

To reduce the pick-up noise in the diamagnetic loop cable, we used a hihgly twisted pair of Teflon cables (two twists per cm cable length, AWG 24 $\hat{=}$ 0.241 mm^2 CU, because in the magnetic environment of ASDEX magnetic field gradients of 0.028 Tesla per cm length are possible /8/). This cable is shielded by a Cu braid (80 % coverage) and an aluminium foil (100 % coverage). The outside diameter of the cable is about 3.5 mm. Cable connectors with small dimensions and constant and very low contact resistance (~1 mΩ) (e.g. Lemo connectors, series B, size 0) are used. As mechanical cable protection we used Teflon tubes and wooden cable ducts.

Both the cable shields and the copper sheets of the diamagnetic compensation loop are grounded on the vacuum vessel (only at the vessel and not in the control room again to prevent ground loops).

5. ELECTRICAL COMPENSATION OF THE DIAMAGNETIC LOOP

After checking the magnetic coupling of the poloidal fields into the diamagnetic loop system during the plasma shots we found that the compensation of the individual poloidal field coil systems is of the order of 10 %. This is true of normal plasma parameter discharges (see Fig. 12). With Rogowski coils /9/ (see Fig. 13) and active integrators we measured the current in the following poloidal field coil systems:

4.9.1 ohmic heating current (J_{OH}max ± 30 kA)
4.9.2 vertical field current ($J_v$max + 45 kA)
4.9.3 divertor coil current (J_{DIV}max + 45 kA)
4.9.4 radial field current ($J_\rho$max ± 1 kA)

For each of these currents a proportional active integrator output voltage is measured and fed into an electronic circuit to add or subtract the compensated diamagnetic signal. To find out the real value of the compensating poloidal field coil signal, we made individual test shots with the

ohmic heating -
vertical yield -
divertor - and
radial field coil systems (see Fig. 12).

By appropriate attenuation of the comparable voltage with a potentiometer the effect of the respective poloidal stray field in the diamagnetic loop signal was nulled. During this test series only the poloidal field of the plasma current itself could not be checked. Since the diamagnetic current always produces a magnetic field opposing the external toroidal field, the polarity of the diamagnetic signal must change sign when the toroidal field is reversed.

For this purpose the polarity and absolute value of the diamagnetic signal were compared in two successive discharges with opposite toroidal field directions but otherwise (as far as possible) identical plasma parameters (n, T_e, T_i). If the diamagnetic coil is correctly compensated, the absolute values of the diamagnetic signal should be the same. Figure 14 plots the diamagnetic signal U_D of the two cases. One has to note that U_D of shot No. 9082 in Fig. 14 is shown inverted. U_D can be calculated as follows:

$$U_D = \frac{\delta\Phi \cdot N_1}{\tau} \tag{23}$$

where τ is the time constant of an active integrator. The equation of the active integrator is given as

$$U_D = \frac{1}{\tau} \cdot \int_0^t U_D' \cdot dt \tag{24}$$

At point A in Fig. 14 the electron densities of the two plasma shots are not equal and therefore the diamagnetic signal of the two shots are not the same during this time. As one can see, in our case we had to compensate for an error of $\Delta\delta\Phi \sim 12$ %.

6. ELECTRICAL CIRCUIT OF THE COMPENSATED DIAMAGNETIC LOOP

Figure 15 shows the flow chart of the electronic circuit used to create the diamagnetic signal $\delta\Phi$.
The voltages induced in the diamagnetic loop ($U'_{COM} + U'_D$) and the voltage induced in the compensating loop ($-U'_{com}$) are added passively at the active integrator No. 1 /10/. With the potentiometer P1 it is possible to calibrate the two induced voltage signals so that any change in the toroidal magnetic field induces no output signal ($\delta\Phi = 0$). With the potentiometer P2 it is possible to add a function to the diamagnetic signal to compensate electronically the flux between the diamagnetic loop and the vacuum vessel.
Apart from the stray field signal Ψ_s, the integrator output signal (Ψ_D) is proportional to the diamagnetic flux:

$$N_1 \cdot \delta\Phi = \int_o^t U'_D \cdot dt = \Psi_D \cdot N_1 = U_D \cdot \tau$$

The active integrator can be triggered (activated) twice before the toroidal field current rises and during the flat-top phase of the toroidal field. The first trigger sets the offset voltage (thermo-voltage) to zero and the second trigger activates the integrator. It is important to maintain the output of the active integrator U_D to less than 10 V during the rise or decrease of the toroidal field to avoid saturation of the integrator.
With the potentiometer P2 the time constant of the vacuum vessel can be electrically adjusted. This compensates the delay of the toroidal field in the vacuum vessel during its rise or fall phase.

With the potentiometer P3 to P6 the effect of the poloidal fields can be adjusted so that any poloidal magnetic field change does not give rise to the signal.
All active integrators of Fig. 15 have an automatic offset control to eliminate thermo-voltage effects created in the wiring of the electric circuits and the drift of the amplifier. Offset voltages of up to 1 mV can be eliminated by this method.

To adjust the potentiometer P3 to P6, we measure the induced stray field signals of all poloidal coils independently, without plasma, at a coil current corresponding to the values during an actual discharge. The stray-field signals partly cancel each other. The stray-field

amplitude Ψ_s is less than 10 % of Ψ_D in a normal plasma discharge, as seen in Fig. 12, where curve 1 shows the diamagnetic signal of a normal plasma shot with neutral injection (dotted area). Curves 2 to 5 show stray-field coupling into the diamagnetic signal without plasma with just the poloidal field currents listed in the table of Fig. 12.

The amount of misalignment with respect to the plasma current was checked by using two consecutive plasma shots with reversed toroidal field directions but otherwise identical plasma parameters. The observed difference in the absolute value of the diamagnetic signal is 25 % and this was also compensated as described above with potentiometer P7.

7. TIME RESOLUTION OF THE DIAMAGNETIC LOOP SIGNAL

We measured the time dependence of the diamagnetic loop signal by creating a fast rising toroidal magnetic field inside the vacuum vessel. A Teflon copper wire with an area of 4 mm^2, 7 windings and a current of about 200 A was used to produce a small toroidal magnetic field just underneath the diamagnetic loop. In Fig. 16 the lower curve shows the time dependence of the current in the test coil system and the upper curve shows the integrated diamagnetic loop voltage $U_D = \frac{\delta \phi \cdot N_1}{\tau}$ From Fig. 16 one can calculate a time constant τ_v of about 15 ms. This measured time constant is mainly the result of the electromagnetic diffusion time constant of the vacuum vessel.

8. COMPUTER PROGRAM (DATA ACQUISITION)

Our data acquisition system consists of a Camac module (ADC 12 bits; ± 5 V, accuracy ± 0.012 %) which makes the analog-to-digital conversion and stores the data of the diamagnetic signal during the plasma discharge with a frequency of 1 kHz (for the normal discharge duration).

After each shot a PDP 11/70 computer reads the Camac module and also handles the Fortran program to calculate $\beta_{p\perp}$ from the stored diamagnetic signal ($U_D \triangleq$ DIA).

With the above-mentioned analysis program we compute and plot the following time-dependent signals as exemplified by shot no. 14067 with

2.4 MW neutral injection during 1.4 to 1.8 s (neutral hydrogen atoms injection in deuterium plasma).

8.1 Plasma current; J_p [kA] (JPLAS 1) see Fig.17

8.2 Toroidal magnetic field; $B_{\phi,TF(0)}$ [T] (BPHI) see Fig.18

8.3 Integrated diamagnetic loop voltage; $U_D[V] \hat{=} \frac{\delta\phi \cdot N_1}{\tau}$ (DIA) see Fig.19

8.4 Calculated beta poloidal; $\beta_{p\perp}[1]$ (BETAP) see Fig.20

$$\beta_{p\perp} = 1 - \frac{8\pi}{2} \frac{B_\phi}{(\mu_o \cdot J_p)^2} \cdot \delta\phi;$$

$$\delta\phi = \frac{U_D \cdot \tau}{N_1}$$

$$\tau = 2[ms]$$

$$N_1 = 2$$

8.5 Safety factor, q [1] (Q) see Fig.21

$$q = \frac{a}{R} \cdot \frac{B_\theta}{B_\phi} = \frac{2\pi}{\mu_o} \cdot \frac{a^2}{R_o} \cdot \frac{B_\phi}{J_p};$$

$$a = 0.4 \text{ [m]}$$

$$R_o = 1.65 \text{ [m]}$$

8.6 Measured loop voltage; U_L [V] (ULOOP) see Fig.22

8.7 Energy confinement time; τ_E[ms] (TAUE) see Fig.23

$$\tau_E[ms] = \frac{\frac{3}{8} \mu_o \cdot R_o \cdot J_p^2 \cdot \beta_{p\perp} \cdot 10^3}{*(U_L \cdot J_p) + P_{NI,P} - \frac{3}{8} \cdot \mu_o \cdot R_o \cdot J_p^2 \cdot \frac{d\beta_{p\perp}}{dt}} \qquad (25)$$

dt → Δt → 5 - 50 [ms] can be chosen in the computer program

* For simplicity we used the measured loop voltage and not the ohmic voltage. For this reason the energy confinement time plots start at the beginning of the flat top of the plasma current (to be exact, 30 kA below J_p max).

8.7.1 Neutral injection power tansferred into the plasma see Fig.24

$$P_{NI,P} = f_{L,H} \cdot P_{NI}\ [MW]\ [(1-e^{-\frac{t}{\tau_s}}) + \frac{0.55 \cdot \tau_1}{\tau_1 - \tau_s}\ (e^{-\frac{t}{\tau_s}} - e^{-\frac{t}{\tau_1}})]\ [MW] \qquad (26)$$

8.7.2 Slowing-down time; electron density $\bar{n}_e$ see Fig.25

$$\tau_s = 10.5\ [ms] \cdot \left[\frac{\bar{n}_e\ [m^{-3}]}{3.5 \cdot 10^{19}}\right]^{0.8}\ [ms] \qquad (27)$$

$$\tau_1 = 35\ [ms]$$

8.7.3 Factor f_L; from the plasma-absorbed neutral injection power during the L-mode

$$f_H = 0.93\ [1 - e^{\frac{-0.66 \cdot \bar{n}_e[m^{-3}]}{10^{19}}}\ [1] \qquad (28)$$

8.7.4 Factor f_H; from the plasma-absorbed neutral injection power during the H-mode

$$f_H = 0.93\ [1 - e^{\frac{-0.66 \cdot \bar{n}_e[m^{-3}]}{10^{19}}}\ [1] \qquad (29)$$

8.8 Toroidal (total) beta; $\bar{\beta} = \bar{\beta}_t$ (BETAT) see Fig. 26

$$\beta = \beta_t = \frac{\beta p_\perp}{q^2 \cdot A^2} \qquad (30)$$

aspect ratio: $A = \frac{Ro}{a} = \frac{1.65\ [m]}{0.4\ [m]} = 4.13\ [1]$

8.9 Correction for $\delta\Phi$ (U_D)

During the plasma shot the vacuum vessel and, therefore, also the diamagnetic loop move radially < 0.1 [mm] toward the centre column because of the centripetal toroidal field forces. This movement creates a flux change in the diamagnetic signal $\delta\Phi$ linear with time. This flux change was measured (see Fig. 27) and the corrections are made in the computer program with the following relation:

$$U_D\ [V] = \underset{\text{(corrected)}}{\frac{N_1 \cdot \delta\Phi\ [Vs]}{\tau[s]}} = \underset{\text{(measured)}}{\frac{N_1 \cdot \delta\Phi\ Vs}{\tau[s]}} - 0.0288\ [\tfrac{V}{s}] \cdot t[s] \qquad (31)$$

A drift of the activated integrator could not be measured if the input was shortened.

9. EXPERIMENTAL TEST RESULTS

9.1 Plasma shot with neutral injection

The plasma shot No. 6357 (Fig. 28) is a high-beta poloidal discharge with the following plasma parameters:

$\beta_{p\perp}$ = 1.22 during neutral injection P_{NI} = 2.1 MW
$\bar{n}_e$ = 3.6 x 10^{13} cm^{-3} before and $\bar{n}_e$ = 4.0 x 10^{13} cm^{-3} during neutral injection
J_p = 370 kA
discharge type: H-mode /3/
neutral injection (neutral hydrogen atoms) between 1.1 and 1.3 s in deuterium (D_2) plasma;
toroidal magnetic field B_ϕ = 2,18 T
divertor discharges without gettering

Figure 28 shows the time-dependent plasma current. Fig. 29 the diamagnetic loop signal U_D (τ = 2 msec). The dotted line is the zero line of the compensated main field (see area C). At area A the diamagnetic signal is not exactly zero because the toroidal magnetic field is still rising during this time. Area B shows the effect in the diamagnetic signal of neutral injection. Figure 30 shows the signal beta poloidal calculated by the computer ($\beta_{p\perp}$).

9.2 Plasma shot No. 4161 with electron density oscillations

Figure 31, curve 3 shows the oscillating electron density ($\bar{n}_e$) measured along a chord through the plasma centre. Curves 1 and 2 are the integrated diamagnetic loop voltage U_D measured with an active integrator at τ = 33 msec. The two curves have gain factors different by a factor of 15, and the diamagnetic signal ($\beta_{p\perp}$) is opposite in phase to the electron density. Beta poloidal increases when the electron density decreases.

9.3 Slide-away discharge, plasma shot 6918

Figure 32 shows a slide-away discharge where three fast gas puffs have been added with an increasing density plateau.

The diamagnetic loop signal $\beta_{p\perp}$ and the plasma position measurement ($\beta_p + l_i/2$) give some information on the shape of the current profile (l_i) and the anisotropy of the distribution function because $\beta_{p\perp}$ is proportional to the perpendicular pressure and $\beta_p + l_i/2$ depends on the weighted sum of the parallel and perpendicular pressures. The results and conclusions from the physical point of view are published in Ref. /11/.

9.4 A 5.7 sec long suprathermal plasma shot with neutral injection

Figure 33 shows the plasma current, Fig. 34 the diamagnetic signal and Fig. 35 the poloidal beta as a function of time for the plasma shot No. 6742. This shot has several different time regions as marked in Fig. 35. During the time region A a normal ohmic heating discharge with a density increase of up to $\bar{n}_e = 3.4 \times 10^{13}$ cm^{-3} is shown. At the time t_1 the gas valve was suddenly closed and the density decreased to $\bar{n}_e = 1.2 \times 10^{12}$ cm^{-3}. During the time region C the loop voltage was only 0.1 volts and a suprathermal plasma was created. Beta poloidal decreases from 0.45 (region A) to 0.13 (region C). During the dotted area (see Fig. 35) neutral injection with a power input into the plasma of 2.4 MW took place. During this time beta poloidal increases from 0.13 to 0.65. This described shot shows that beta poloidal is not very strongly dependent on the plasma current. In region B the plasma current changes several times from ~250 kA to ~300 kA (see Fig. 33).

SUMMARY

We have shown that beta poloidal can be reliably measured down to values of 0.1. Care has to be taken in the mounting of the diamagnetic loop and the cable routing. It is very important to consider the design of the diamagnetic loop and the cable routing during the design phase of the plasma device.

We have shown that it is possible to install a diamagnetic loop during the mounting of a plasma device at a fixed position and compensate later for magnetic stray fields electronically.

It is very convenient with known diamagnetic flux signal ($\delta\Phi$),

plasma current (J_p), loop voltage (U_L) and toroidal magnetic field ($B_{\phi,TF}$) to calculate and plot by computer beta poloidal ($\beta_{p\perp}$), the energy confinement time (τ_E) and beta toroidal (β_t) versus time without knowing T_e, T_i and n_e.

ACKNOWLEDGEMENTS

The authors wish to thank Dr. O. Klüber for his support on the theoretical part of this paper. We thank R. Allgeyer and S. Schraub for the design of the diamagnetic loop. The skillful technical assistance of H.J. Berger, J. Franzspeck, P. Matern, K. Sahner and H. Steidl is gratefully acknowledged. They are grateful to P. Luttner for the support on the electronic circuitry and E. Karl for writing the computer program. They thank T. Henningsen for taking the photographs and H. Volkenandt for preparing the drawings. Many thanks to Dr. F. Dylla, Dr. E. Meservey, A.M. Nicol, Dr. A. Stäbler and Dr. F. Wagner for critically reading the manuscript.

NOTE: Reference to a company product or name does not imply approval or recommendation of the product by IPP to the exclusion of others that may be suitable.

REFERENCES

/1/ MUKHOVATOR, V.S., SHAFRANOV, V.D., Nuclear Fusion 11 (1971), p. 605 to 633, Plasma Equilibrium in a Tokamak.

/2/ The ASDEX Group, IPP-Report III/47 (1978), Divertor Tokamak ASDEX.

/3/ WAGNER, F., et al., Phys. Rev. Lett. 49, No. 19, p. 1408-1412 (1982), Regime of Improved Confinement and High Beta in Neutral-Beam-Heated Divertor Discharges of the ASDEX Tokamak.

/4/ FUSSMANN, G., et al., Phys. Rev. Lett. 47, p. 1004 - 1007 (1981), Long Pulse Suprathermal Discharges in the ASDEX-Tokamak.

/5/ HAEGL, M., and SAND, F., Plasma Physics, Vol. 17, No. 11 (1975), Compensated coil system for measuring the plamsa diamagnetism in toroidal devices.

/6/ WHITE, D., A Handbook on electromagnetic shielding materials and performance. Don White Consultants, State Route 625, P.O. Box D, Gainesville, Virginia 22065 (USA).

/7/ WHITE, D., Electromagnetic interference and compatibilty, Vol. 3, Don White Consultants, State Route 625, P.O. Box D, Gainesville, Virginia 22065 (USA).

/8/ GERNHARDT, J., et al., IPP Report III/67 (not finished yet), Low noise cable for diagnostic, control and instrumentation for the fusion experiment ASDEX (Tokamak).

/9/ GERNHARDT, J., et al., IPP Report III/65 (1981), An Equipment Protection and Safety System for the ASDEX Tokamak (with a description to measure very high D.C. currents with active integrators).

/10/ GROENING, D.E., IPP Report III/63 (Dec. 1980).

/11/ FUSSMANN, G., et al., 9th International Conference on Plasma Physics and Controlled Nuclear Fuson Research, Baltimore USA, 1-8 Sept. 1982, Paper IAEA-CN-41/W-1, Investigation of suprathermal discharges in the ASDEX tokamak.

APPENDIX: DEFINITIONS (SI UNITS)

INDEX $\parallel$ parallel to the toroidal magnetic field $B_{\phi,TF}$

INDEX $\perp$ perpendicular to the toroidal magnetic field $B_{\phi,TF}$

a [m]	minor plasma radius (a ~ 0.40 m) at the boundary
$A = R_o/a$ [1]	aspect radius
A [m^2]	area
A_{cu} [mm^2]	copper area of an electrical cable
A_{COM} [m^2]	flux area of compensating diamagnetic loop
A_D [m^2]	flux area of diamagnetic loop
B_D [T]	magnetic field created by diamagnetic current
B_θ [T]	poloidal magnetic field
$B_\theta(1)$ [T]	poloidal magnetic field at the plasma boundary (r = a), (ρ = 1)
B_ϕ [T]	total toroidal magnetic field (created by the toroidal field coils and the diamagnetic effect of the plasma)
$B_{\phi,TF(0)}$ [T]	toroidal magnetic field created by the toroidal field coils at the plasma centre (ρ = 0; R_o = 1.65 m)
f_L [1]	from the plasma-absorbed neutral injection power during the H-mode
f_H [1]	from the plasma-absorbed neutral injection power during the L-mode
h [mm]	height of compensated diamagnetic loop segment
J [A]	current
J_D [A]	diamagnetic current
J_{DIV} [A]	divertor coil current
J_{OH} [A]	ohmic heating coil current
J_p [A]	plasma current
J_v [A]	vertical field coil current
J_ρ [A]	radial field coil current
$k = 1.38 \cdot 10^{-23}$ $[\frac{J}{mol \cdot K}]$	Boltzmann constant
$k' = 1.52 \cdot 10^{-16}$ $[\frac{Ws}{keV}]$	Boltzmann constant
l_i [1]	inner plasma inductivity
n [m^{-3}]	plasma density
n_e [m^{-3}]	electron density
n_{eo} [m^{-3}]	electron density at the plasma centre

n_i [m^{-3}]	ion density
n_{io} [m^{-3}]	ion density at the plasma centre
$N_1 = 2$ [1]	number of windings of the diamagnetic measuring loop
$N_2 = 37$ [1]	number of windings of the compensating diamagnetic loop
$< P >$	kinetic plasma pressure (average over the plasma column cross-section)
P_{NI} [MW]	neutral injection power of the injector
$P_{NI,P}$ [MW]	neutral injection power transferred into the plasma
q [1]	safety factor of tokamak
r	minor plasma radius
R [m]	radial direction
$R_o = 1.65$ [m]	large plasma radius
t [s]	time
T_e [keV]	electron temperature
T_{eo} [keV]	electron temperature at the plasma centre
T_i [keV]	ion temperature
T_{io} [keV]	ion temperature at the plasma centre
U [V]	voltage
U'_{COM} [V]	voltage induced in the compensation loop
U'_D [V]	voltage induced in the diamagnetic loop
U_D [V]	voltage proportional to the diamagnetic flux $\delta\Phi$
U'_{DIV} [V]	voltage induced in the Rogowski coil of the divertor coil system
U_L [V]	loop voltage of ASDEX
U'_{OH} [V]	voltage induced in the Rogowski coil of the ohmic heating coil system
U'_p [V]	voltage induced in the Rogowski coil for the plasma current
U'_s [V]	voltage induced by stray fields
U'_v [V]	voltage induced in the Rogowski coil of the vertical field coil system
U'_ρ [V]	voltage induced in the Rogowski coil of the radial field coil system
W [mm]	width of compensating diamagnetic loop
Z [m]	vertical direction
α [1]	exponent
$\beta = \beta_t$ [%]	total beta (beta toroidal); plasma pressure ratio

β_p [1]	poloidal beta (average over the plasma column cross-section)
$\beta_{p\perp}$ [1]	perpendicular component of beta poloidal (average over the plasma column cross-section)
γ [1]	exponent
$\delta\phi$ [Vs]	diamagnetic flux (created by the plasma itself)
$\delta\phi_s$ [Vs]	diamagnetic flux created by stray fields only
ΔH [cm]	horizontal displacement of the plasma centre ($\Delta H > 0$; outward)
$\ominus$ [°]	poloidal direction
$\mu_o = 4 \cdot \pi \cdot 10^{-7}$ $[\frac{Vs}{Am}]$	permeability of free space
$\pi = 3{,}14$ [1]	
$\rho = r/a$ [1]	relative radius
τ [s]	time constant of active integrator for diamagn. signal ($\tau = 2 \cdot 10^{-3}$ s)
τ_1 [ms]	time constant of the neutral injection power
τ_E [ms]	energy confinement time of the plasma
τ_s [ms]	slowing-down time
τ_v [ms]	time constant of the stainless-steel vacuum vessel ($\tau_v \sim 10$ ms)
ϕ [°]	toroidal direction
ϕ [Vs]	total toroidal flux
ϕ_{TF} [Vs]	toroidal flux created only by the toroidal field winding
Ψ [Vs]	flux
$\Psi_D = \delta\phi$ [Vs]	diamagnetic flux
Ψ_{DIV} [Vs]	flux proportional to the divertor coil current
Ψ_{OH} [Vs]	flux proportional to the ohmic heating coil current
Ψ_p [Vs]	flux proportional to the plasma current
Ψ_s [Vs]	stray flux
Ψ_v [Vs]	flux proportional to the vertical field coil current
Ψ_ρ [Vs]	flux proportional to the radial field coil current

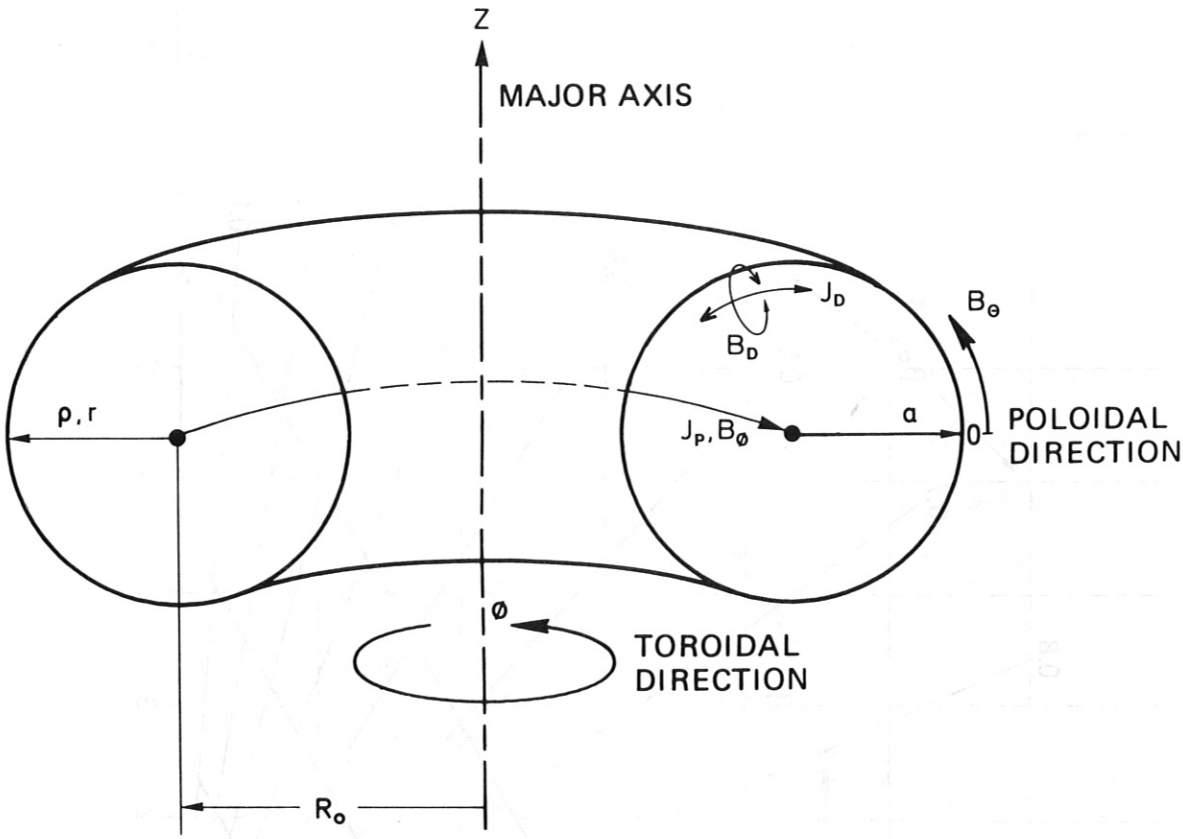

Fig. 1: Geometrical parameters. Plasma ring carrying a longitudinal current.

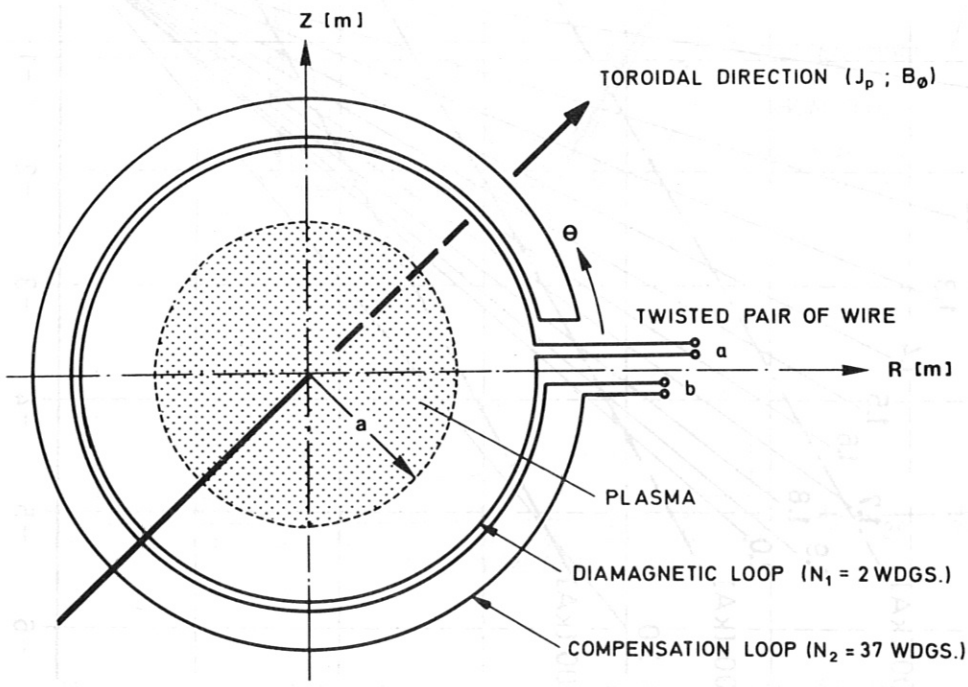

Fig. 2: Schematic of a diamagnetic loop and a compensating loop.

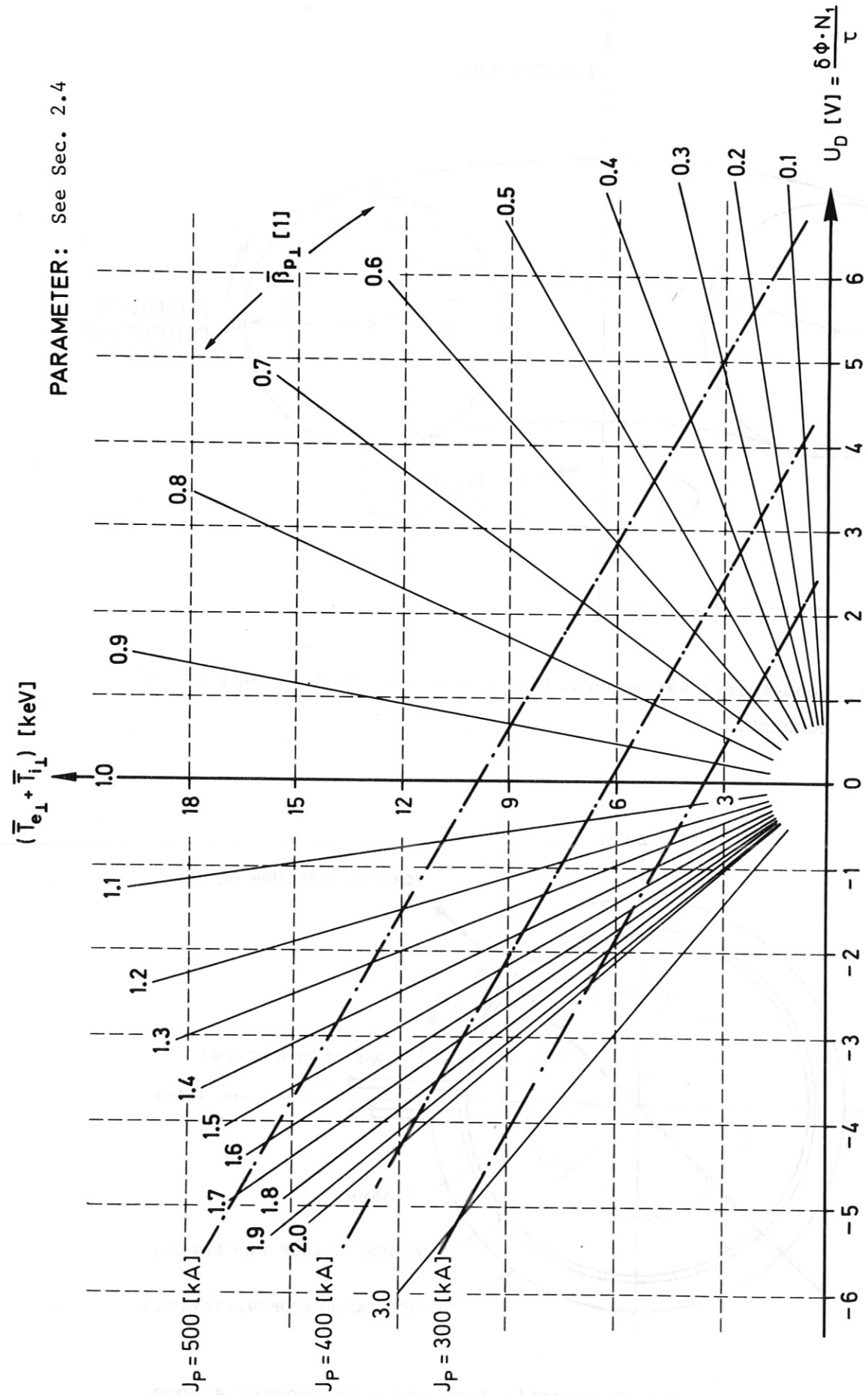

Fig. 3: Numerical relations for the ASDEX diamagnetic loop.

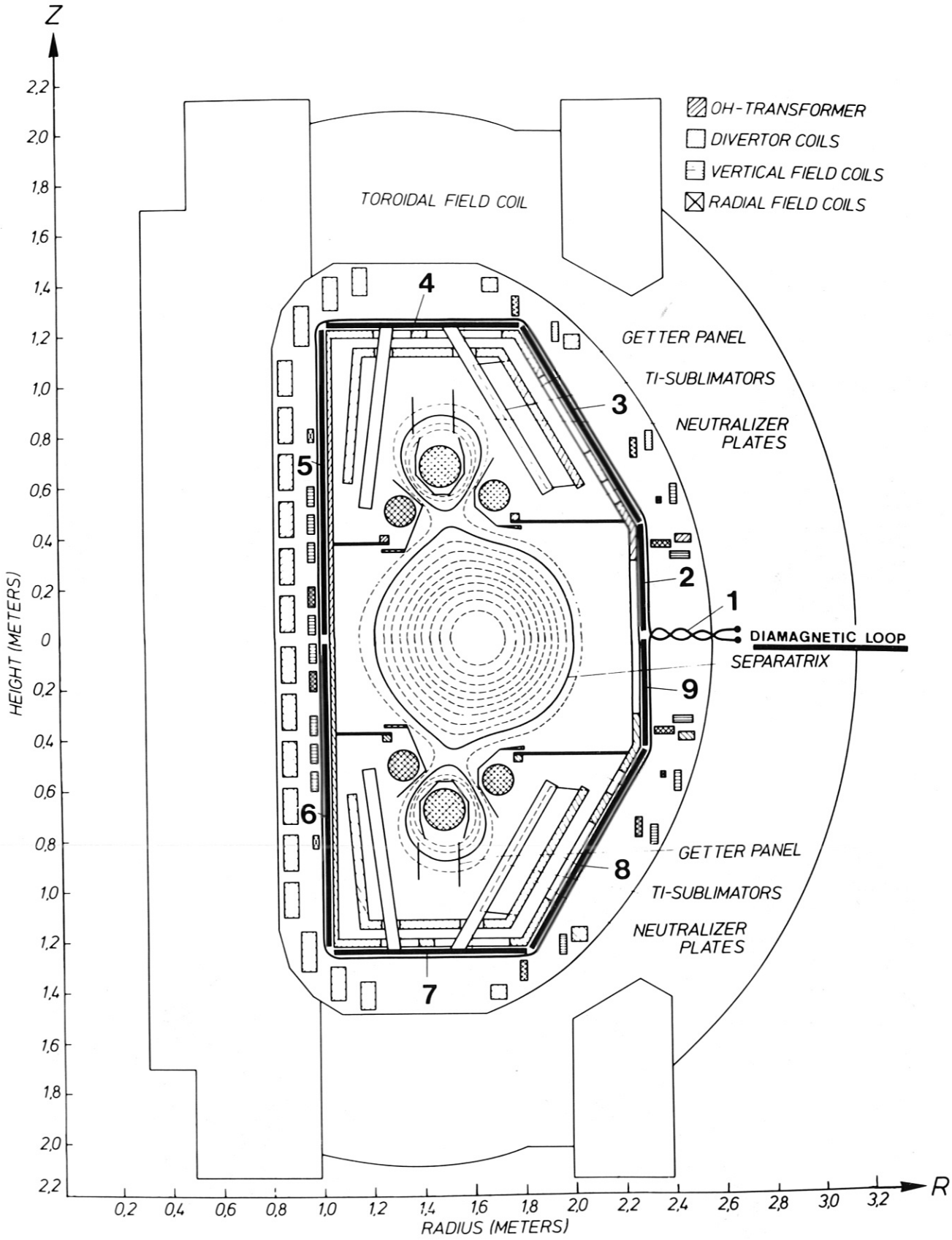

Fig. 4: The ASDEX stainless-steel vacuum vessel, poloidal and toroidal field coils, and the diamagnetic loop no. 1 and the compensation loop section no. 2 to 9.

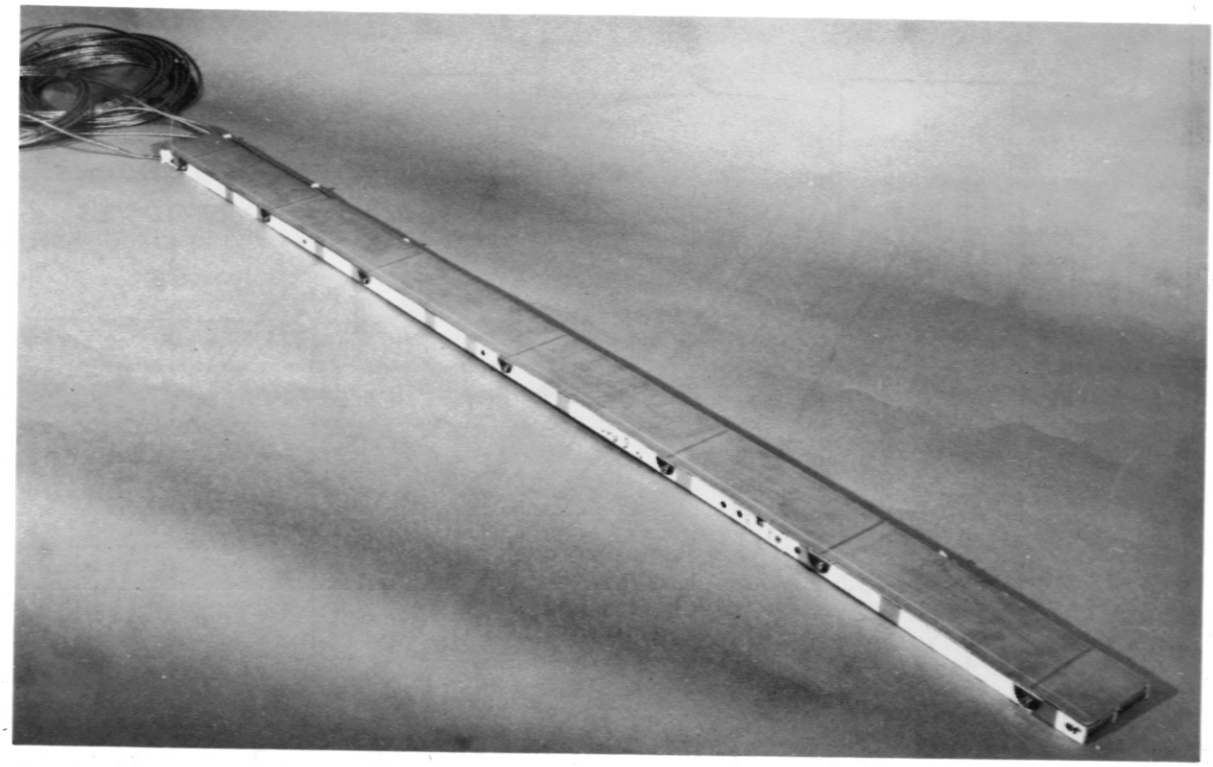

Fig. 5a: Phtotgraph of the compensation loop section no. 6 (see Fig. 4). Top view.

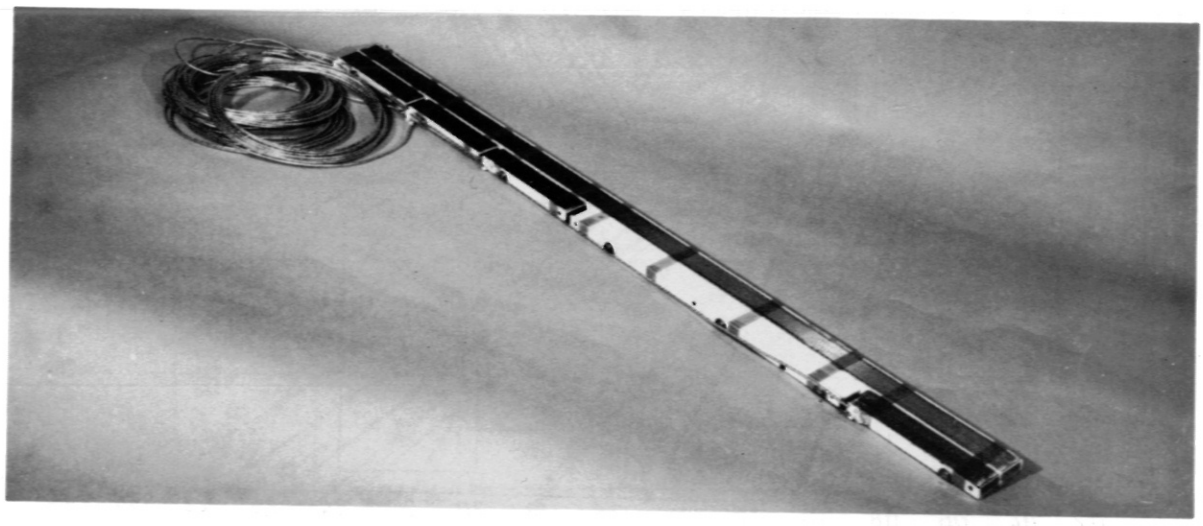

Fig. 5b: Photograph of the compensation loop section no. 6 (see Fig. 4). Bottom view.

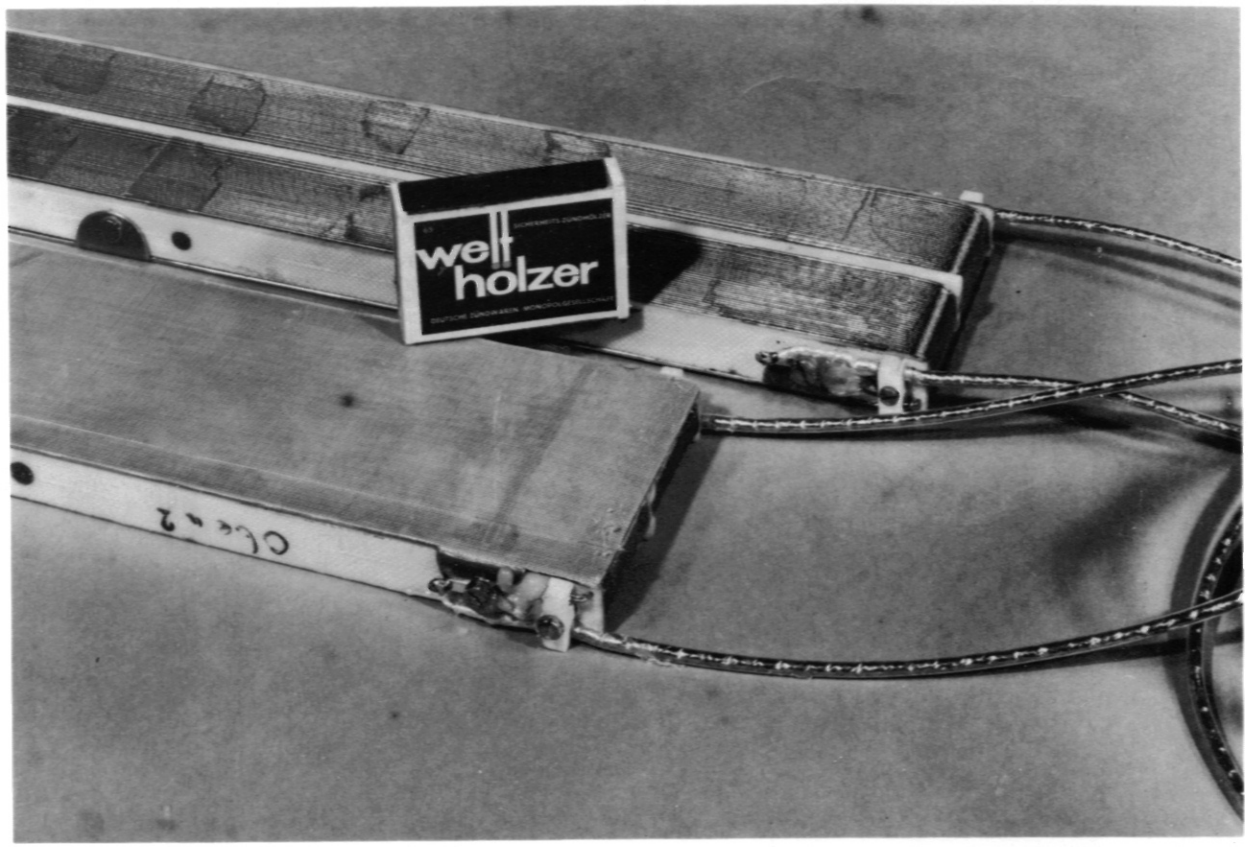

Fig. 6: Photograph of the compensation loop section no. 5 unshielded and section no. 6 shielded with cables (see Fig. 4). Match-box for reference.

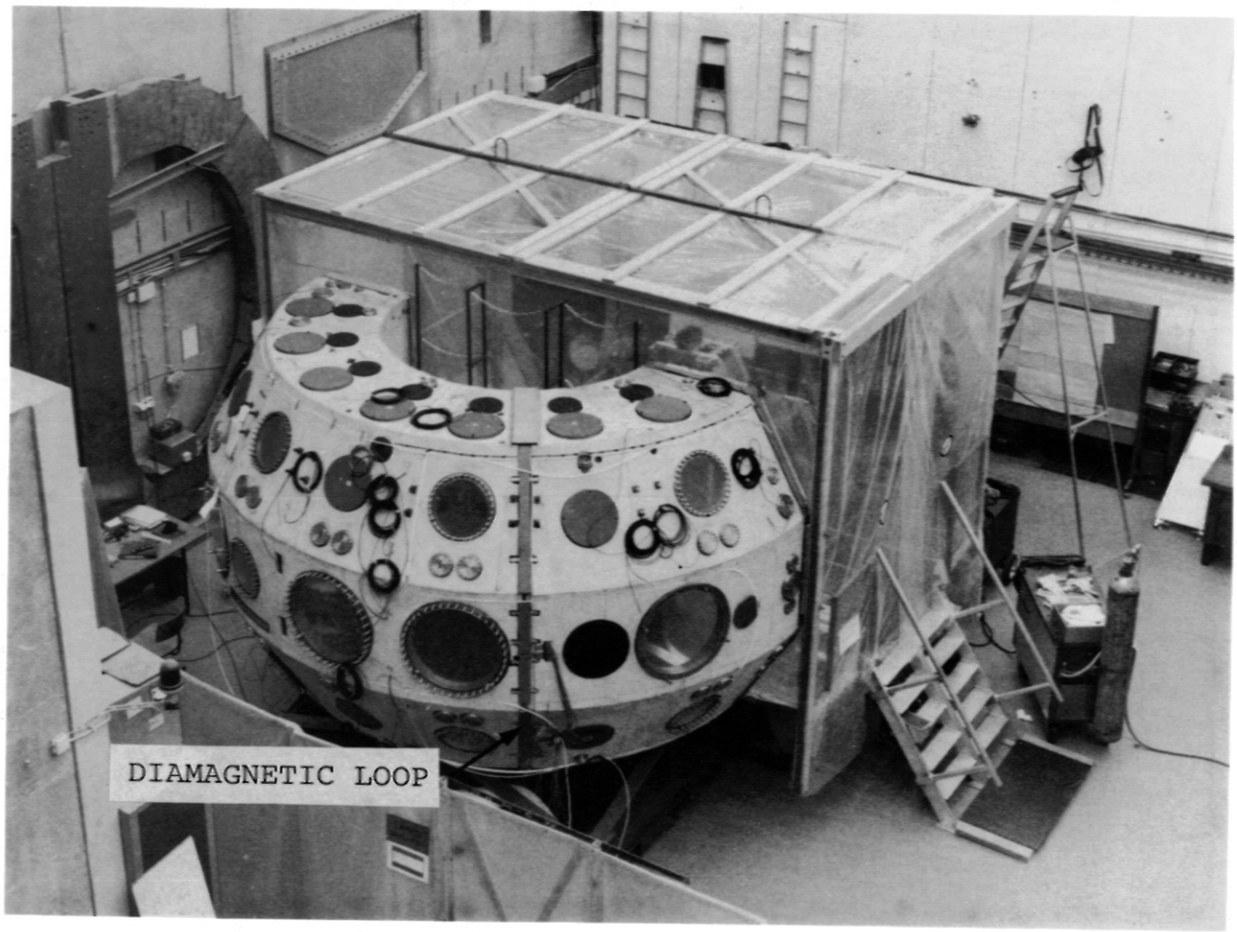

Fig. 7: Photograph of one half of the ASDEX stainless-steel vessel with the mounted diamagnetic loop (outside view).

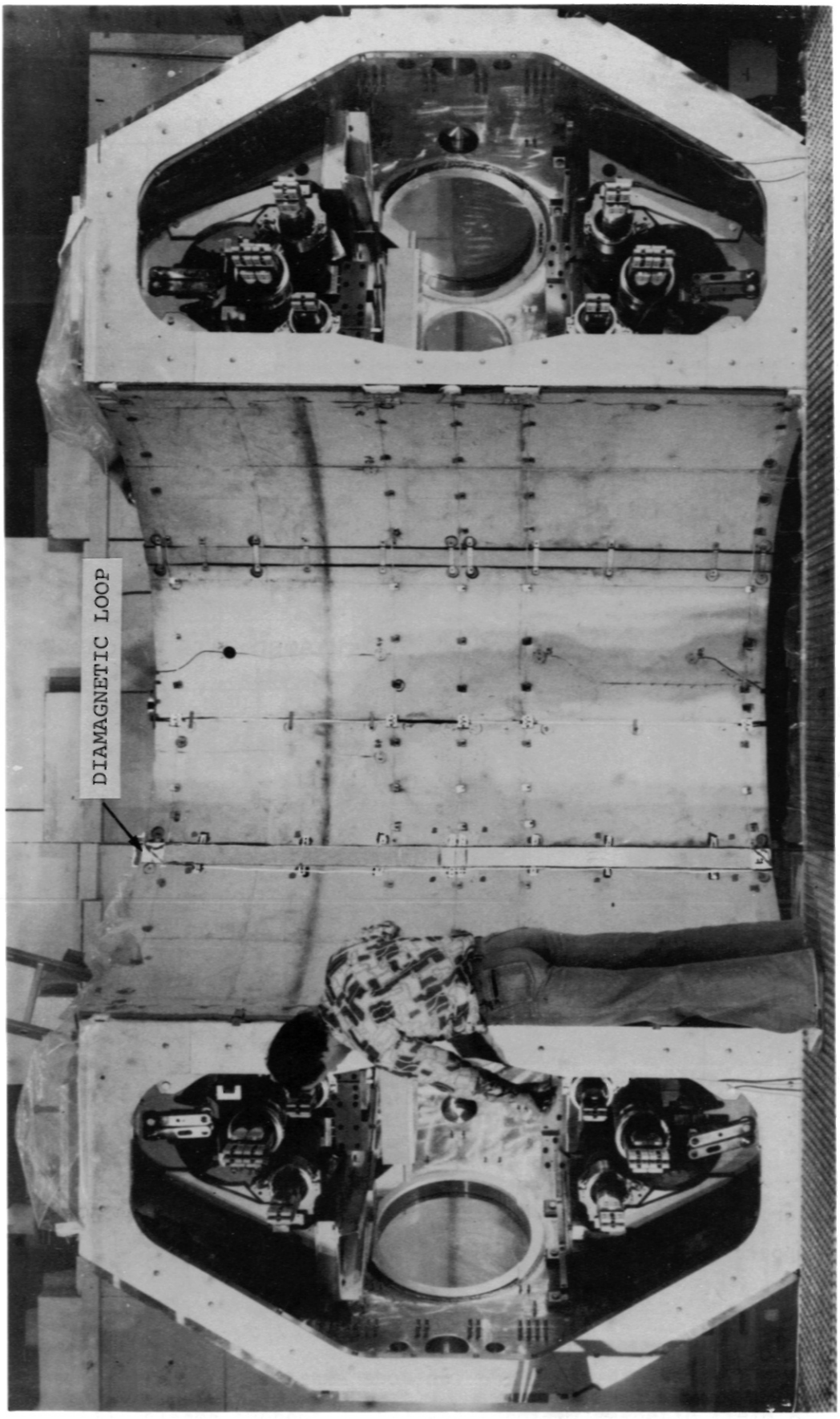

Fig. 8: Photograph of one half of ASDEX stainless-steel vessel with the mounted diamagnetic loop (inside cylinder).

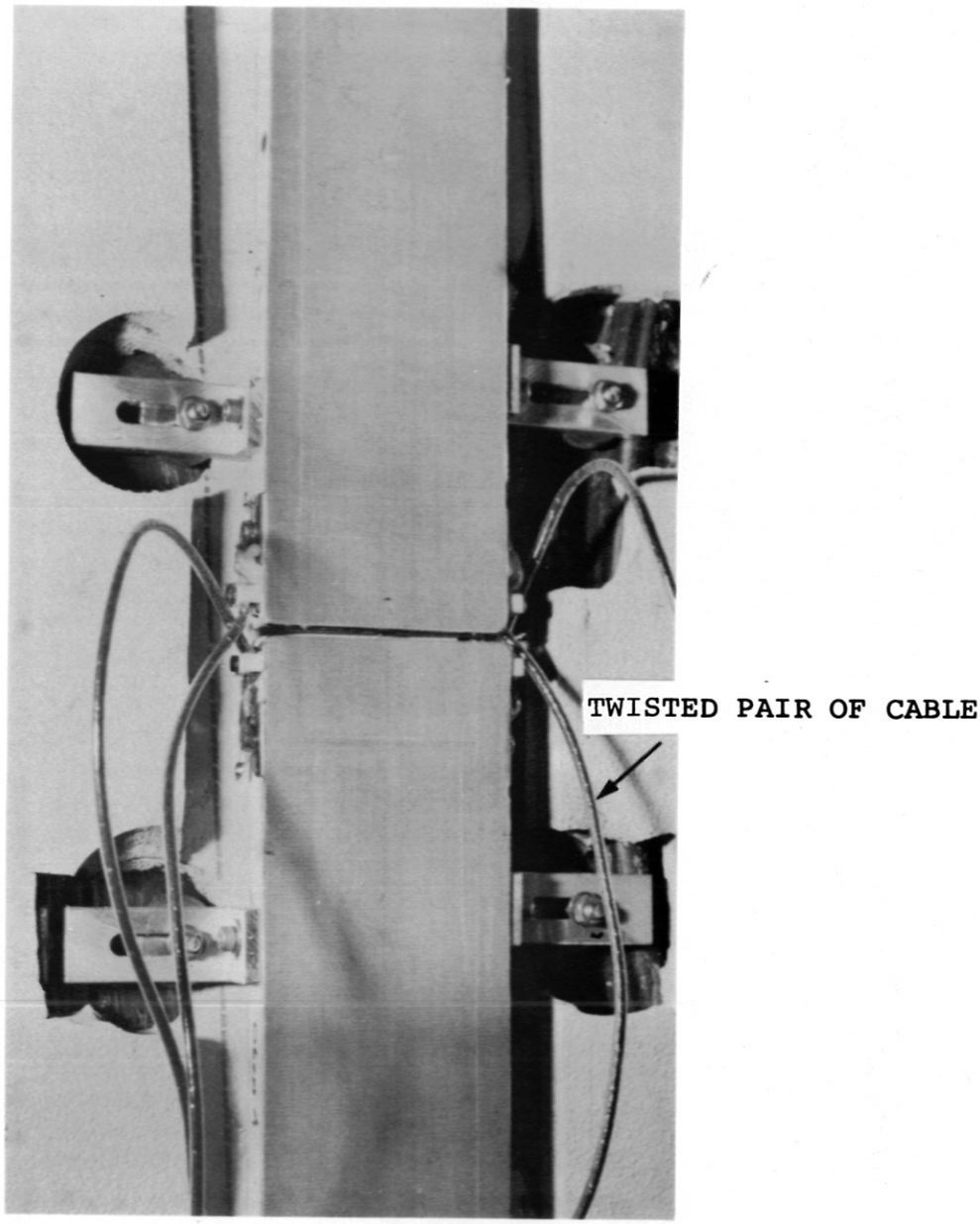

Fig. 9: Micrometer screw adjustment of compensating loop section no. 5 (upper) and section no. 6 (lower) (see Figure no. 4).

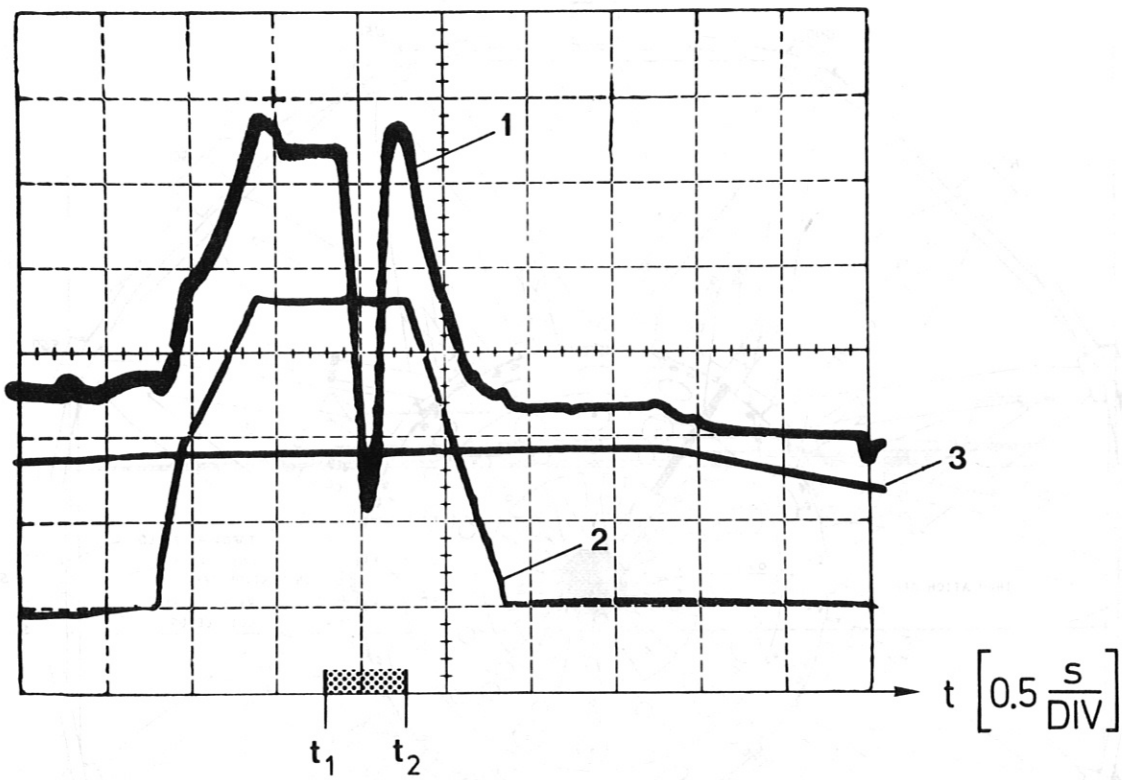

CURVE 1: DIAMAGNETIC SIGNAL; U_D ; $1\left[\frac{V}{DIV}\right]$; τ = 2 [ms]

CURVE 2: PLASMA CURRENT; J_p; $1\left[\frac{V}{DIV}\right] \cdot 100\left[\frac{kA}{V}\right]$

CURVE 3: TOROIDAL MAGNETIC FIELD; $B_{\phi,TF(O)}$ = 2,18 [T]

BETWEEN t_1 and t_2 NEUTRAL INJECTION (2.4 MW)
SHOT No. 6655.
$\bar{n}_e = 3.6 \times 10^{13}$ [cm^{-3}]

Fig. 10: Oscillogram of plasma shot no. 6655 with diamagnetic signal U_D (1), plasma current J_p (2) and toroidal magnetic field $B_{\phi,TF}$ (3).

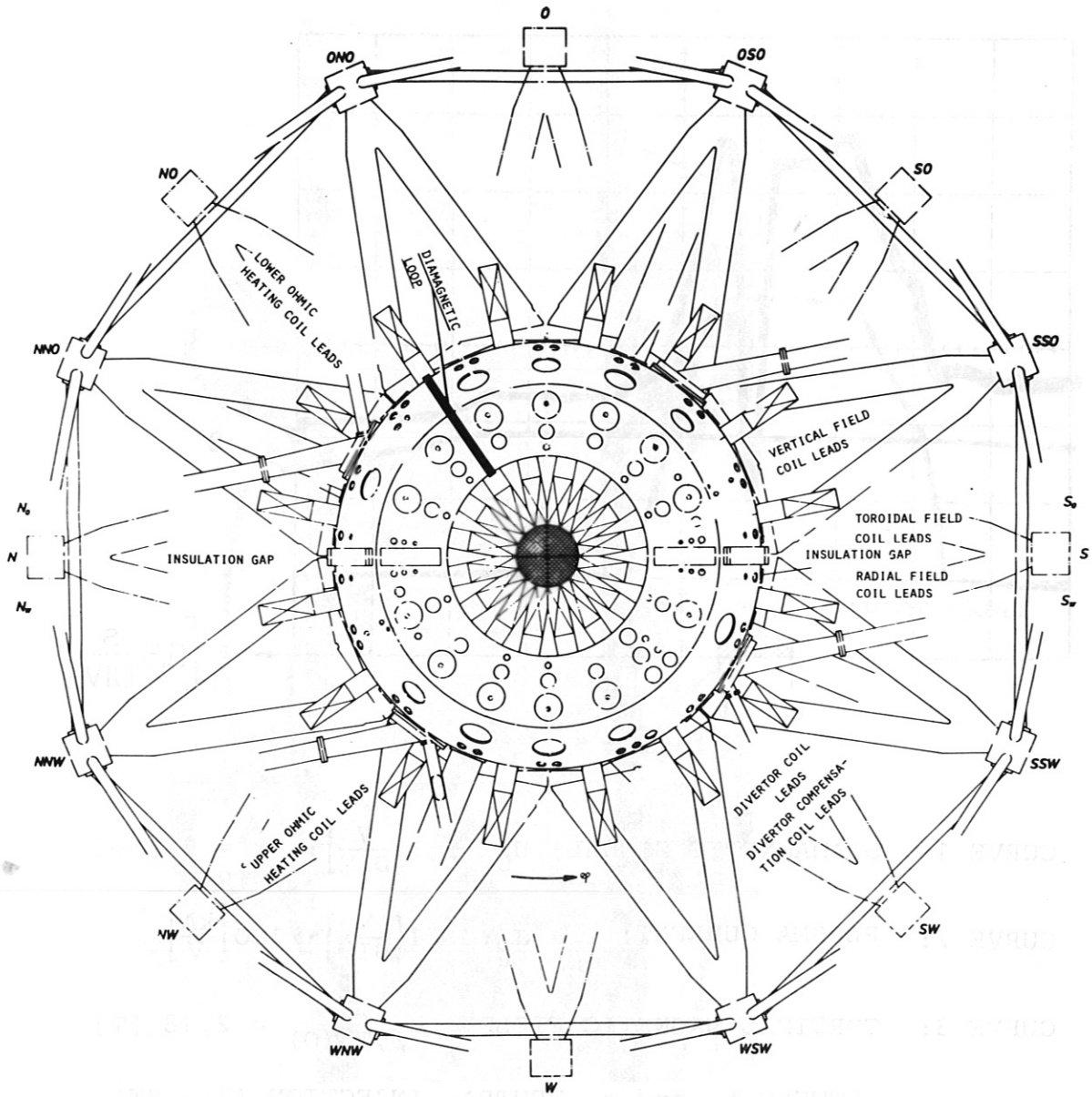

Fig. 11: Mounting of the diamagnetic loop in a noise-free area (top view of ASDEX).

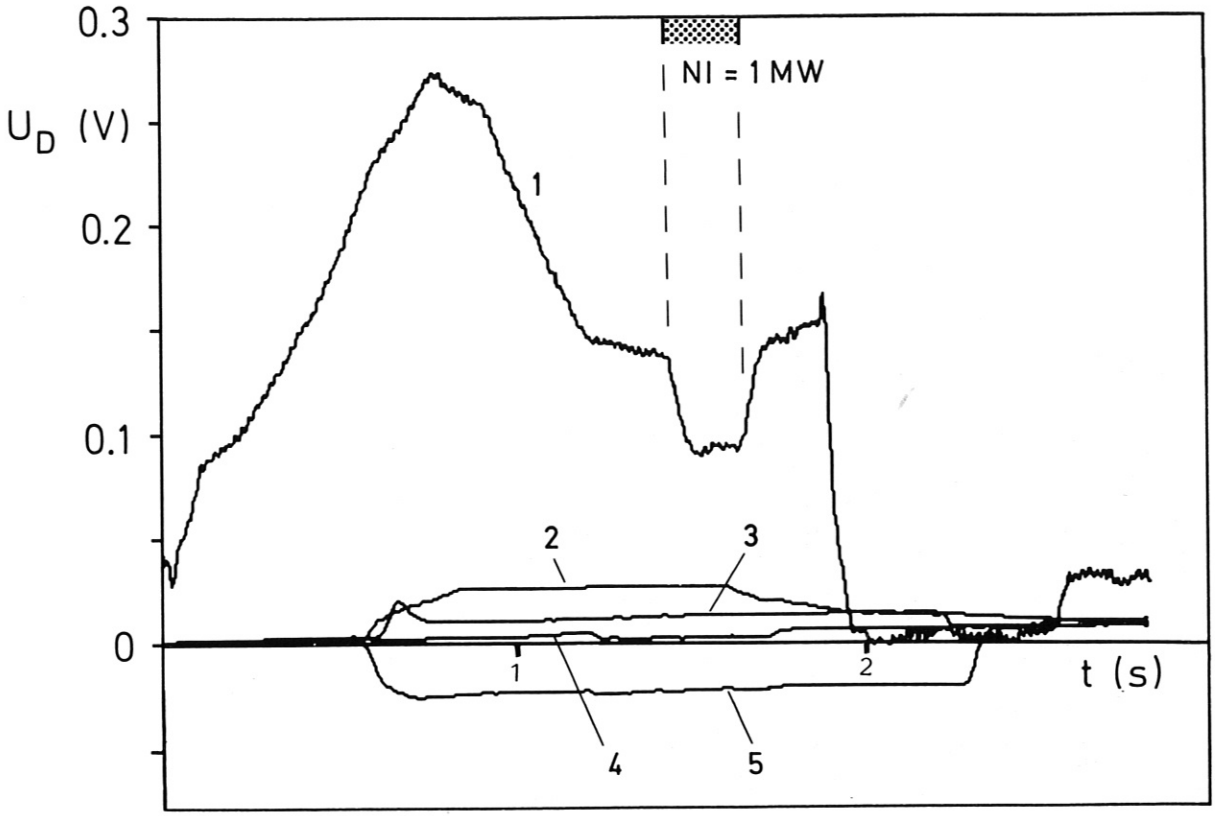

curve No.	signal name U_D = DIA[V]	gain [1]	remarks	shot No.
1	DIA	10	plasma shot	4146
2	DIA	10	ohmic heating current only; J_{OH} =20 [kA]	53
3	DIA	10	vertical field current onlv; Jv =20 [kA]	55
4	DIA	10	divertor coil current only; J_{DIV} =20 [kA]	60
5	DIA	10	radial field current only; J_p = 1 [kA]	61

time constant of active integrator τ = 33 [ms]
diamagnetic loop: number of windings N_1 = 2

Fig. 12: Diamagnetic signal U_D during the plasma shot No. 4146 (curve 1) and the coupling of poloidal magnetic fields into the diamagnetic loop (curve 2 to 5).

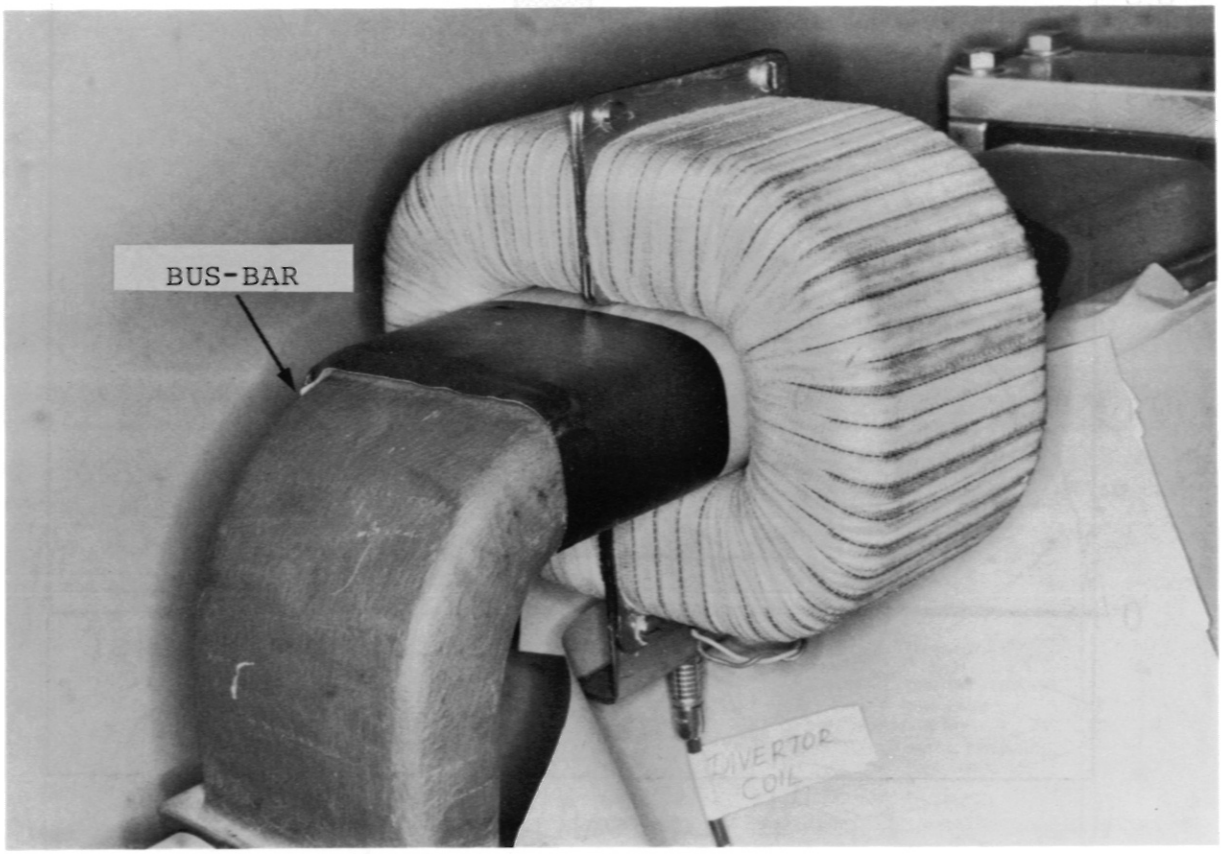

ROGOWSKI COIL:

TOTAL NUMBER OF WINDINGS	800
NUMBER OF LAYERS	2
COIL AREA	A = 2750 [mm^2]
COIL BODY MATERIAL:	PLYWOOD
BUS-BAR OPENING:	40 x 85 [mm]

WIRE: KAPTON INSULATED COPPER WIRE
AWG 30 ≙ 0,057 [mm^2] Cu
OUTSIDE DIAMETER: 0.55 [mm]

THE ROGOWSKI COIL CONSISTS OF TWO PARTS SCREWED TOGETHER.

LEMOSA CONNECTOR WITH TWISTED PAIRS.

Fig. 13: Rogowski coil to measure divertor coil current (see photograph), ohmic-heating, radial-field, and vertical-field currents.

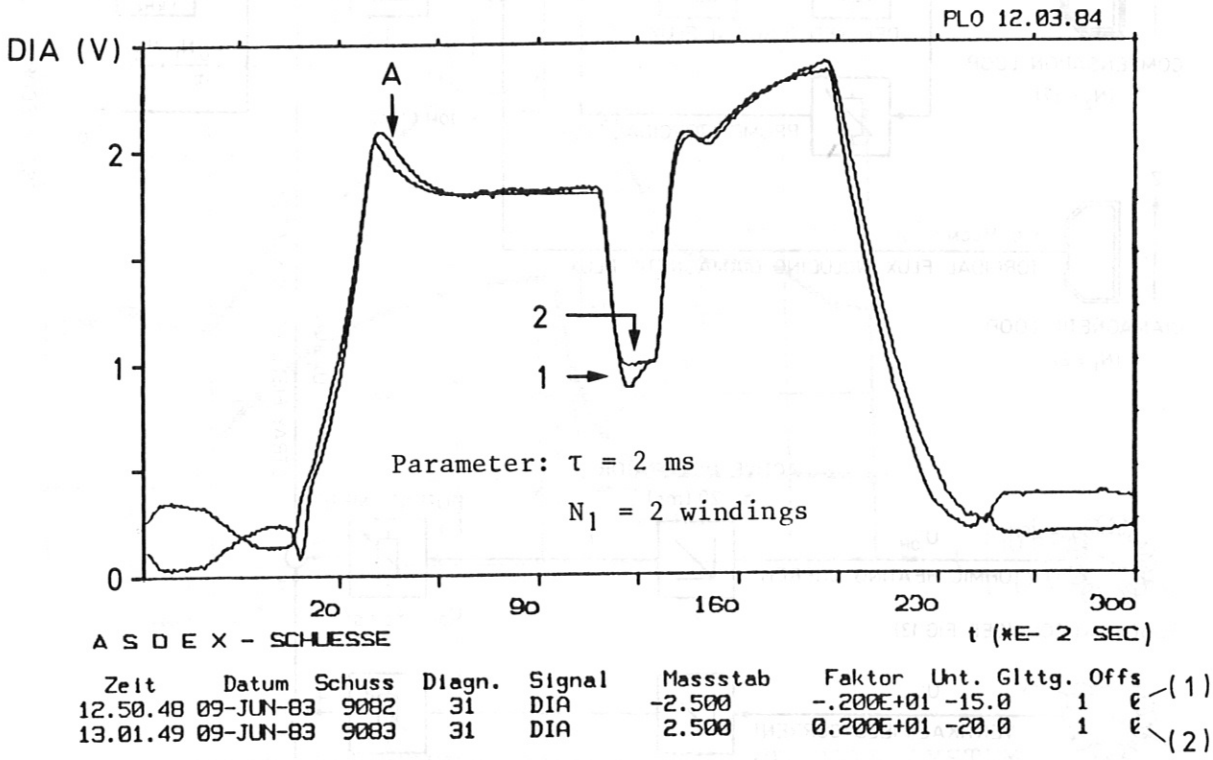

Fig. 14: Diamagnetic signal U_D during plasma shot no. 9082 with negative toroidal field and plasma shot no. 9083 with positive toroidal field. The plasma current flow in both shots was in the positive direction (positive direction ≙ mathematically positive direction).

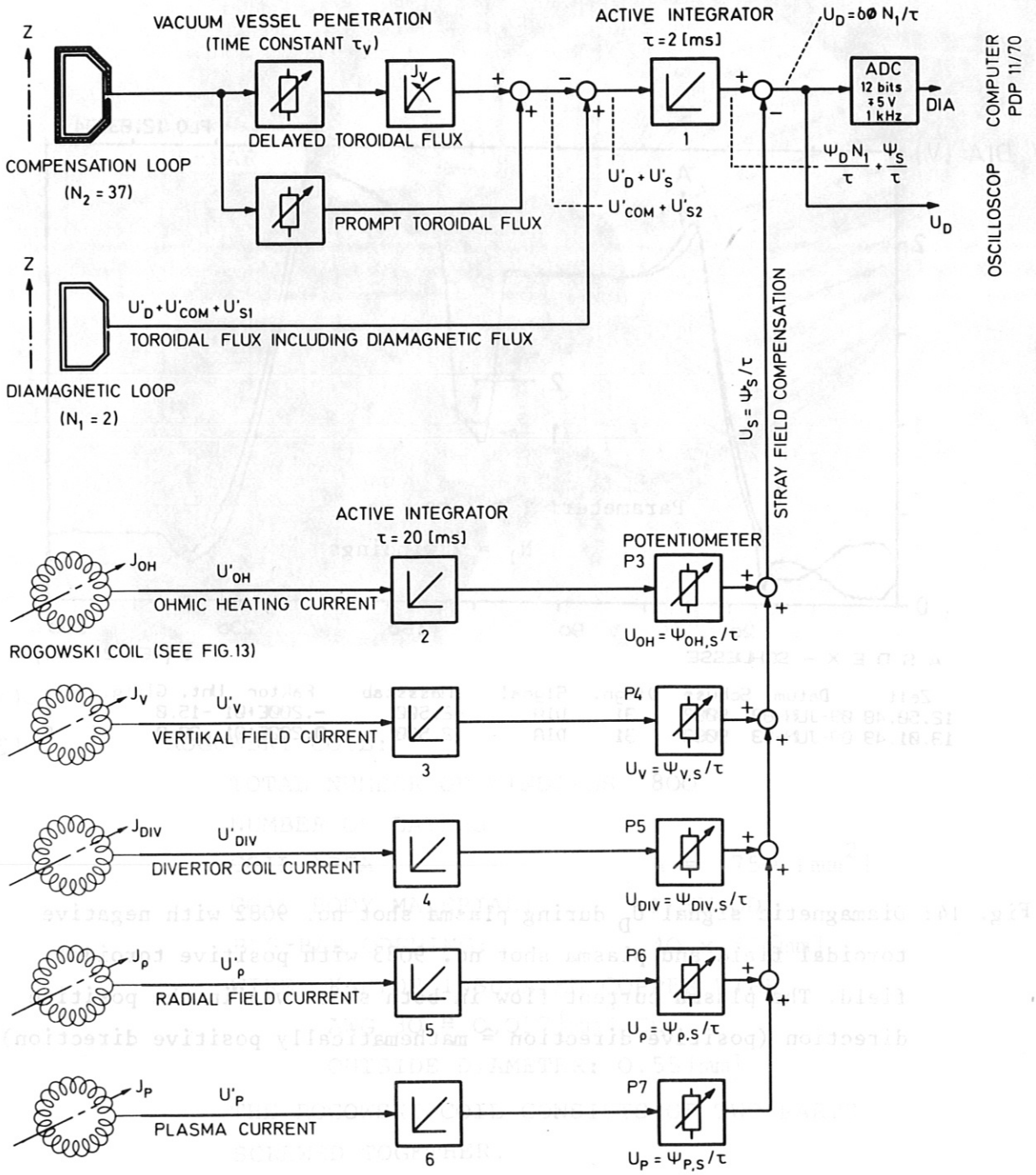

Fig. 15: Flow chart of the electronic circuit of the diamagnetic signal measurement.

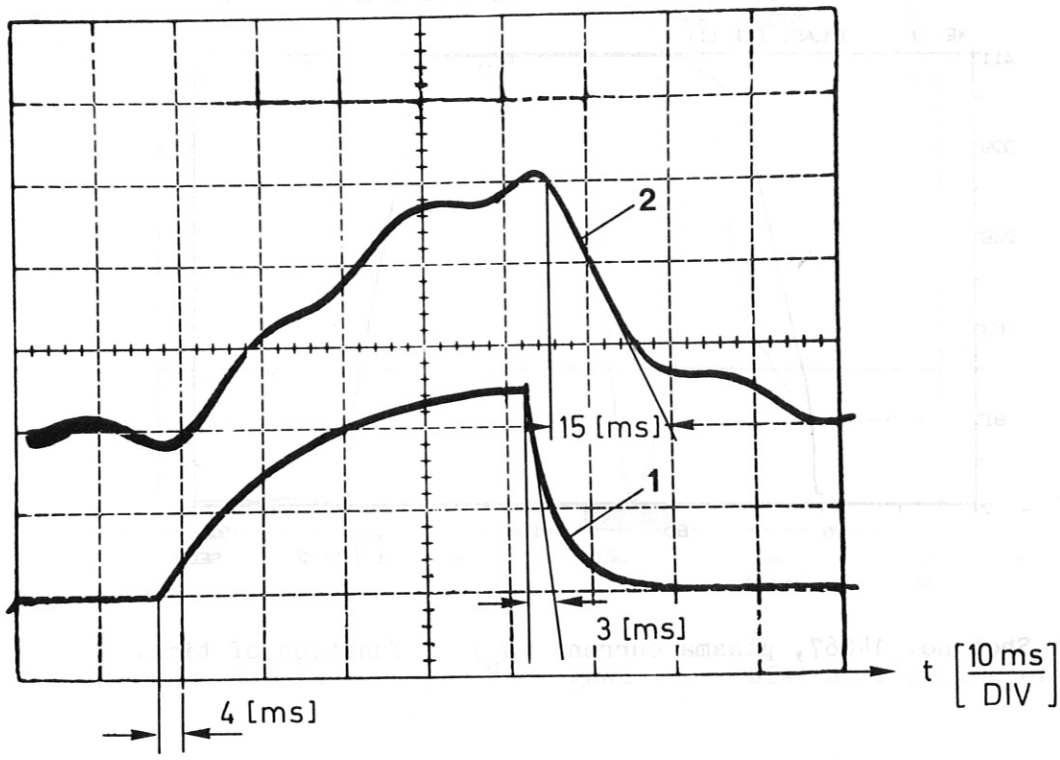

CURVE 1: CURRENT FLOWING IN THE COIL SYSTEM MOUNTED INSIDE THE STAINLESS STEEL VESSEL FOR TEST PURPOSE.

$$J = 20\ [\frac{mV}{DIV}] \times \frac{100\ [A]}{30\ [mV]}$$

CURVE 2: DIAMAGNETIC SIGNAL; U_D [V] INDUCED BY THE CURRENT J.
TIME CONSTANT OF ACTIVE INTEGRATOR,
τ = 33 [ms].
SENSITIVITY OF CURVE 2 10 $[\frac{mV}{DIV}]$

Fig. 16: Oscillogram of the time resolution of the diamagnetic loop.

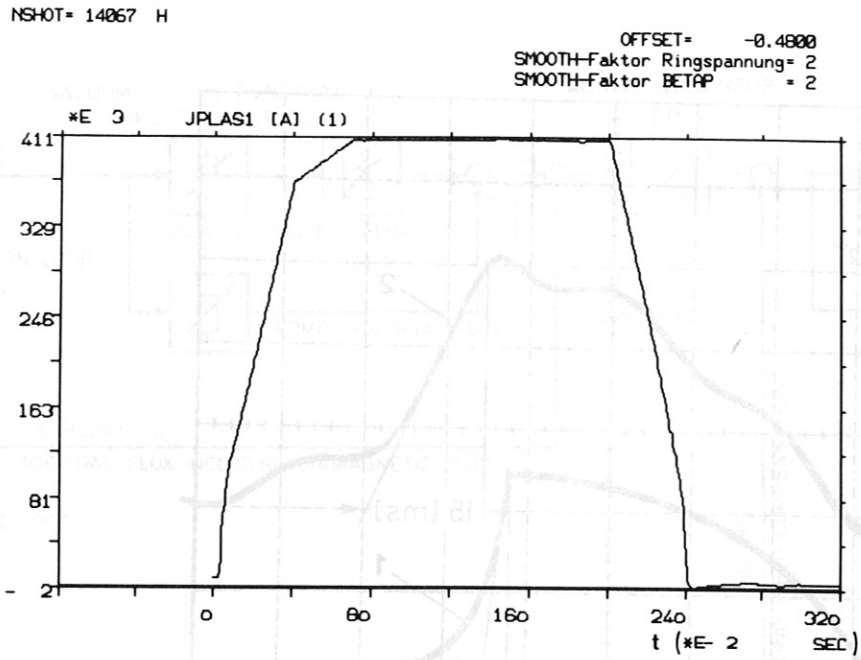

Fig. 17: Shot no. 14067, plasma current (J_p) as function of time.

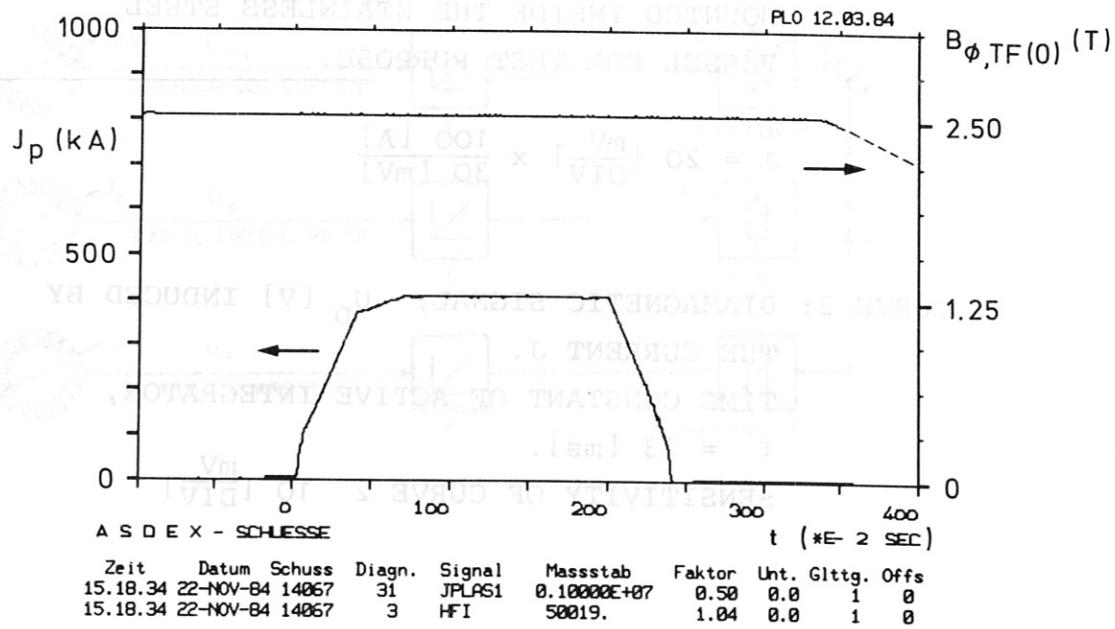

Fig. 18: Shot no. 14067, plasma current (J_p) and toroidal magnetic field $B_{\phi,TF(0)}$ as function of time (full scale 5 seconds).

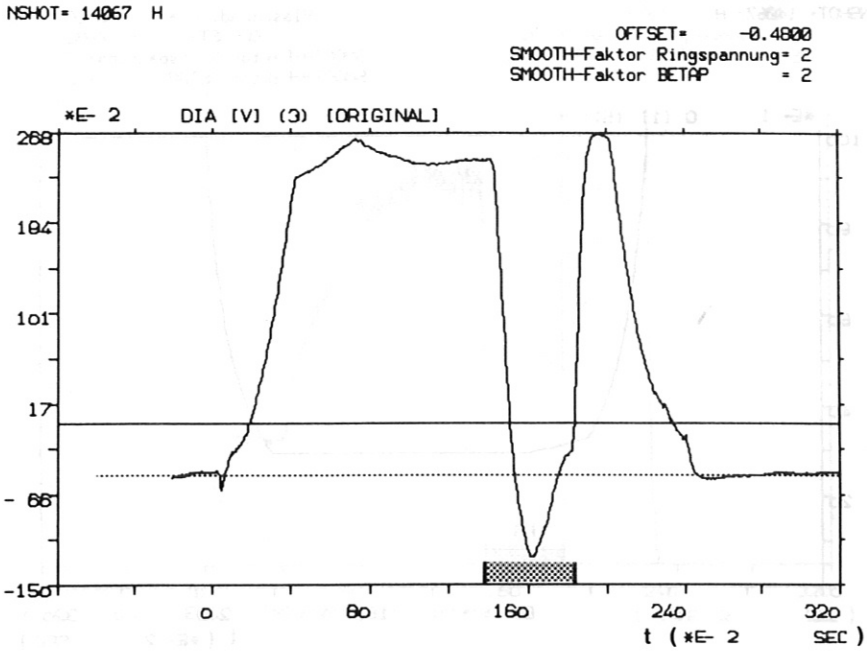

Fig. 19: Shot no. 14067, diamagnetic signal (U_D = DIA) as function of time.

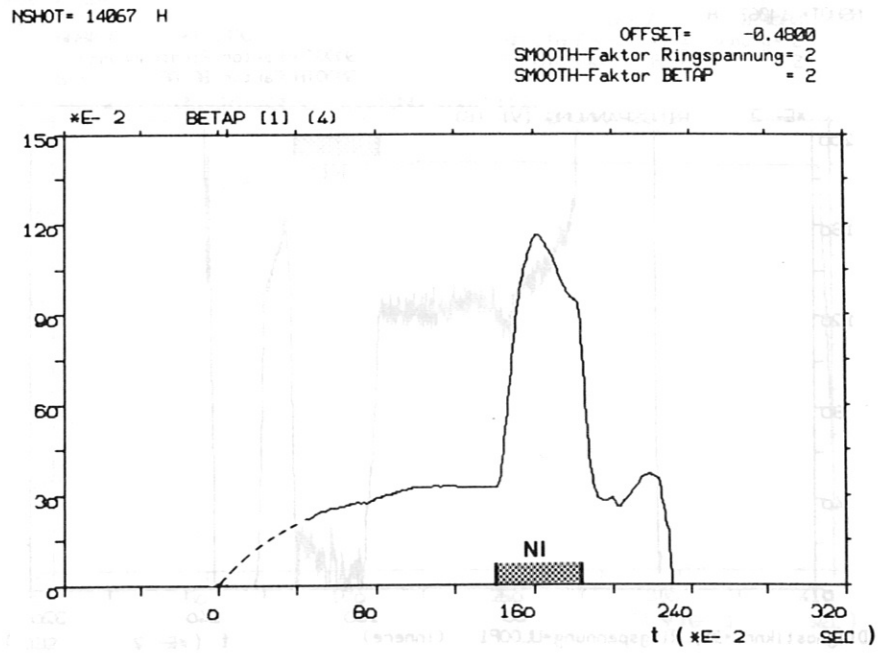

Fig. 20: Shot No. 14067, beta poloidal ($ß_{p\perp}$ = BETAP) as function of time.

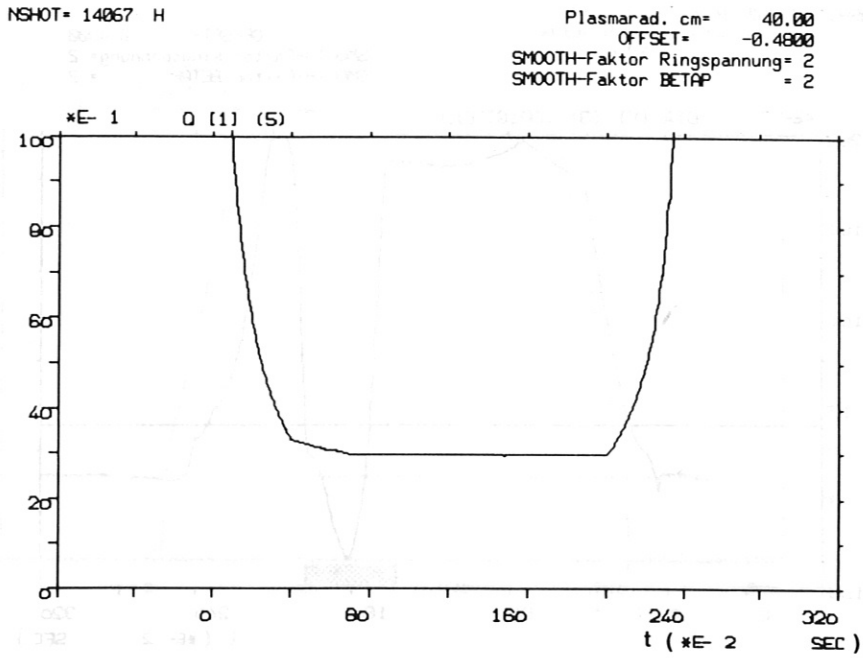

Fig. 21: Shot no. 14067, stabilisation factor (q = Q) as function of time.

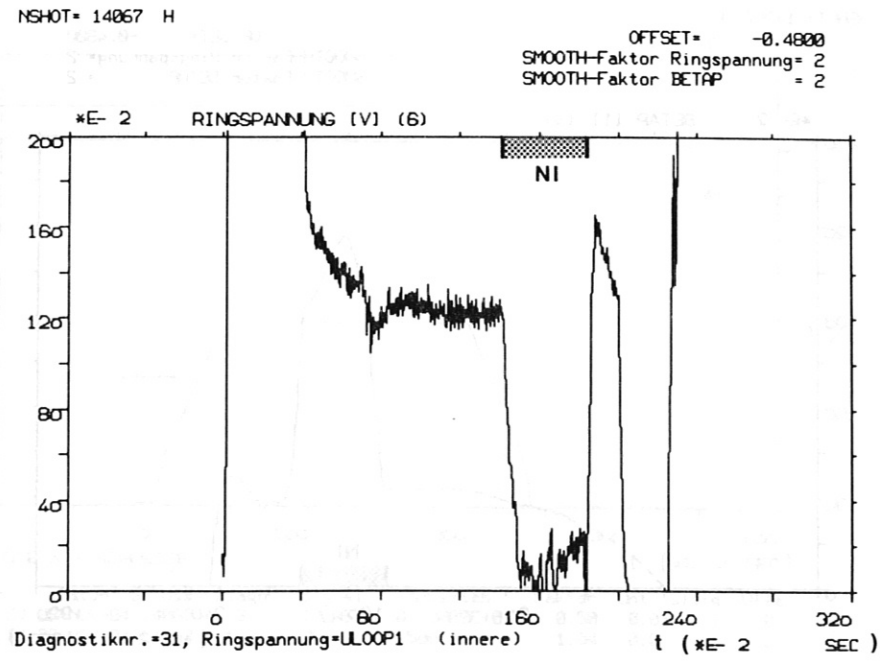

Fig. 22: Shot no. 14067, loop voltage (U_L) as function of time.

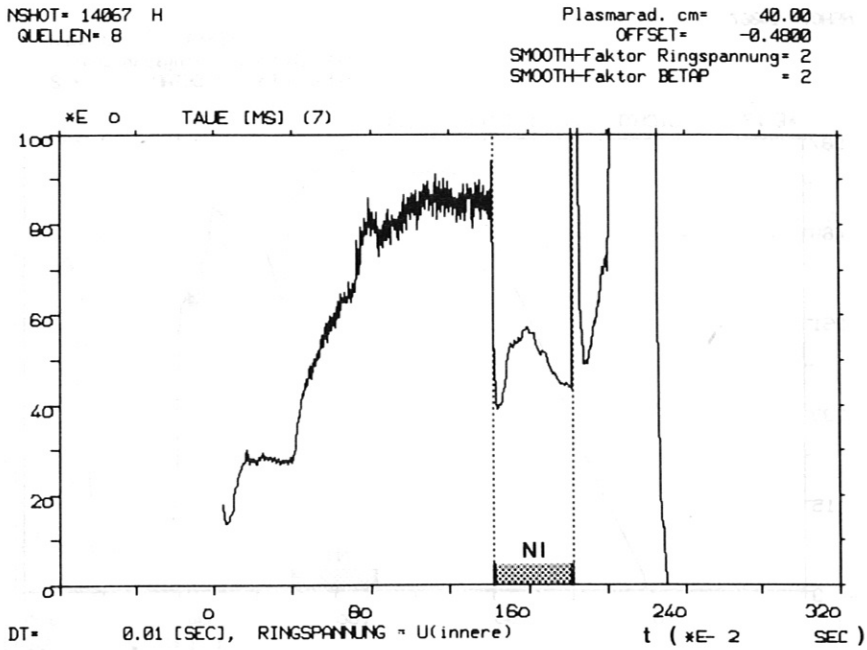

Fig. 23: Shot no. 14067, energy confinement time (τ_E = TAUE) as function of time.

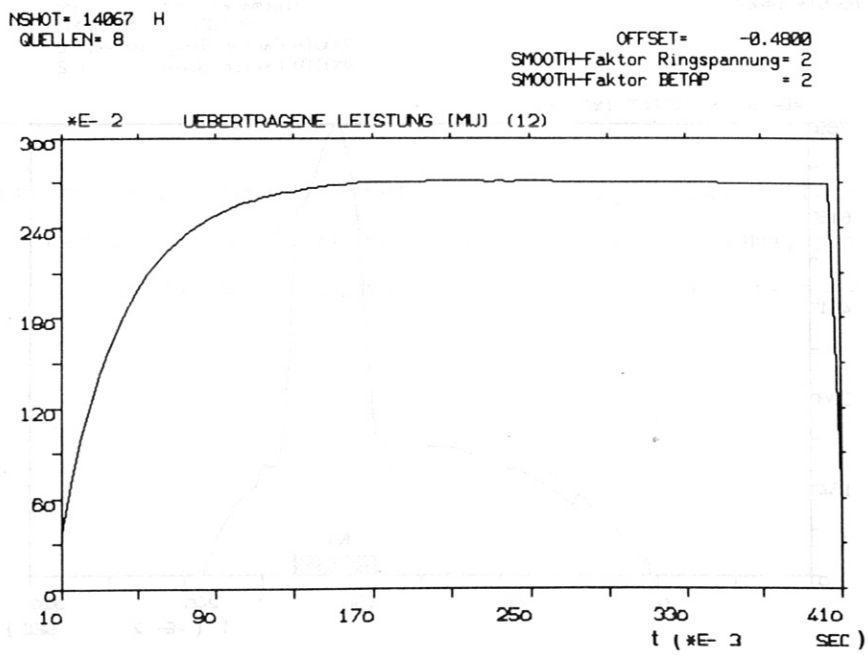

Fig. 24: Shot no. 14067, neutral injection power ($P_{NI,P}$) transferred into the plasma as function of time.

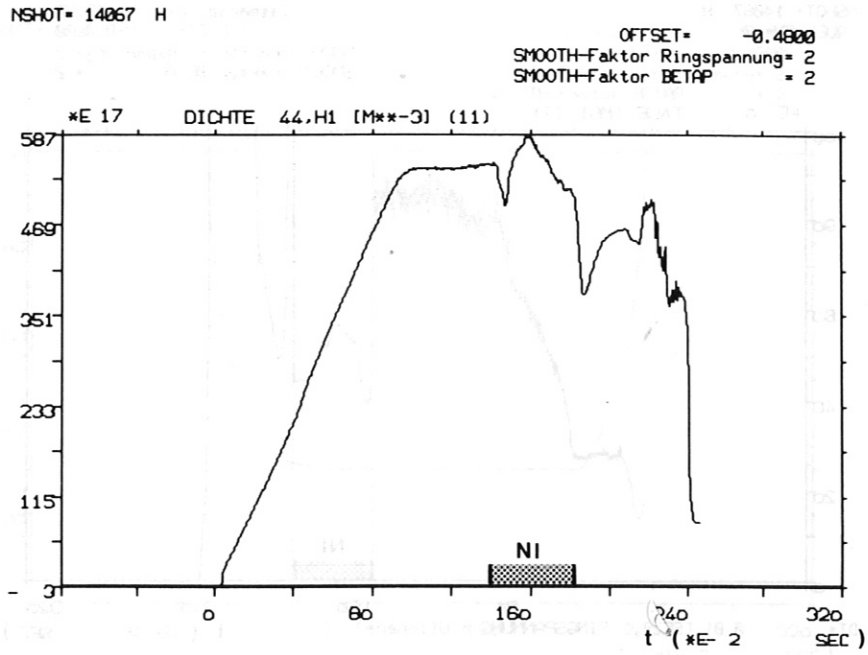

Fig. 25: Shot no. 14067, electron density ($\bar{n}_e$) as function of time.

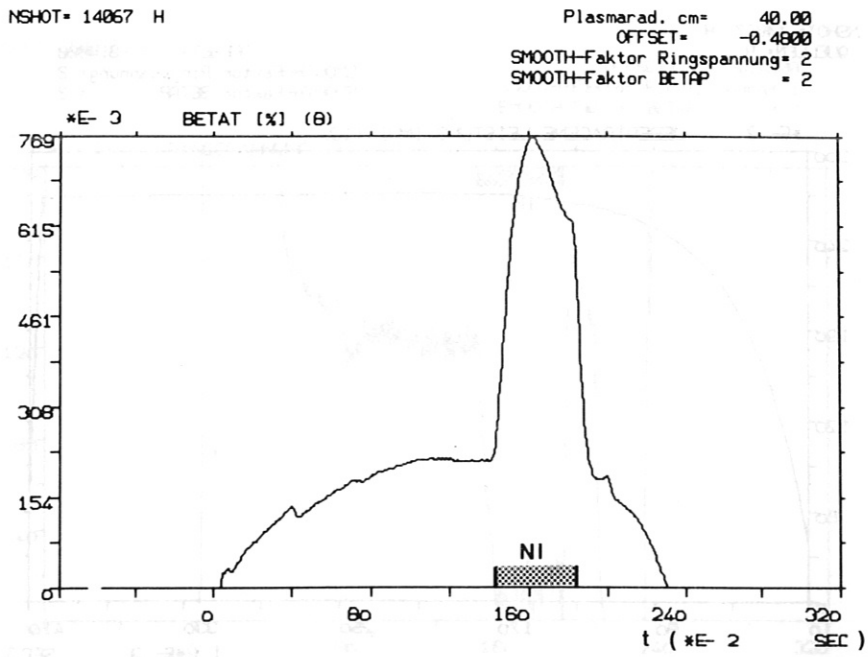

Fig. 26: Shot no. 14067, toroidal beta (β_t = BETAT) as function of time.

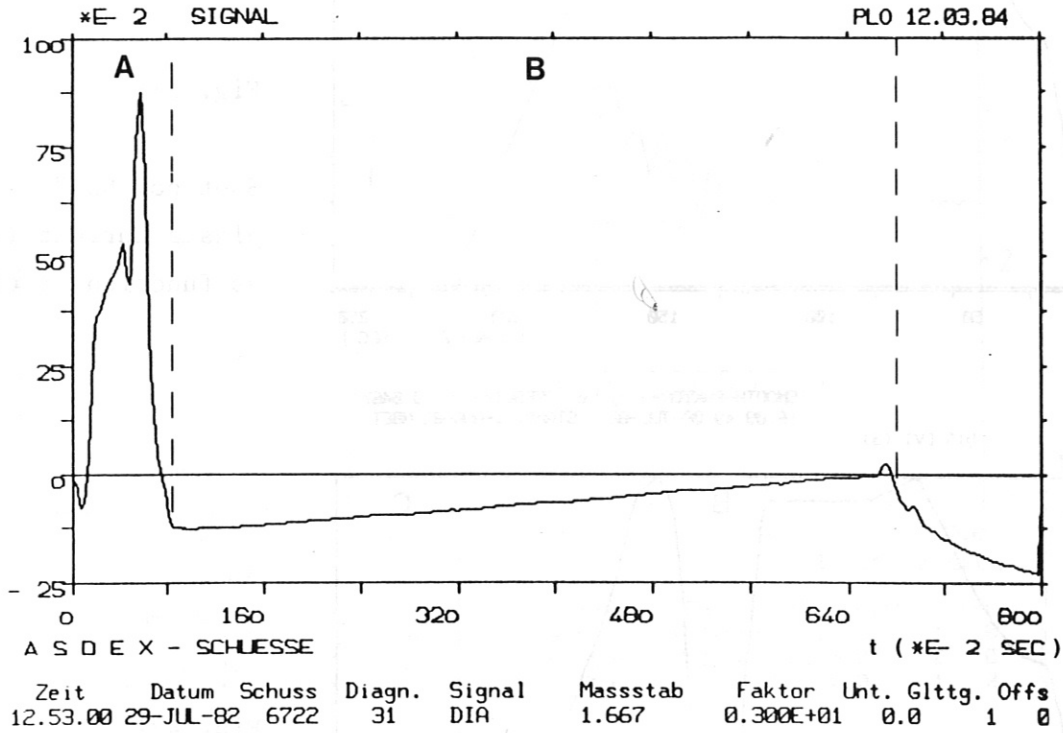

Fig. 27: Change in the diamagnetic signal (U_D = DIA) as function of time. Part A of the curve is shown with plasma, part B without plasma but with constant toroidal magnetic field of 2.2 tesla.

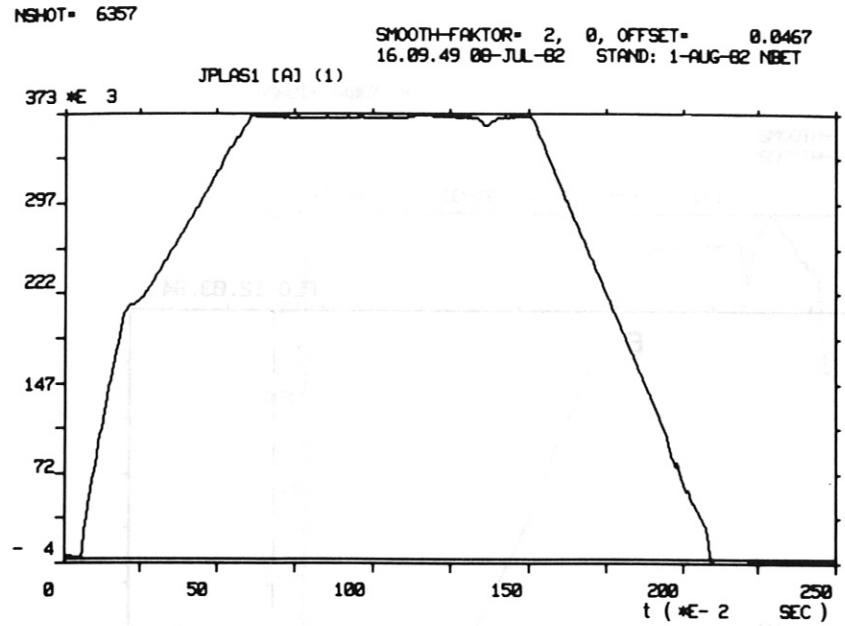

Fig. 28:

Shot no. 6357,
plasma current (J_p)
as function of time.

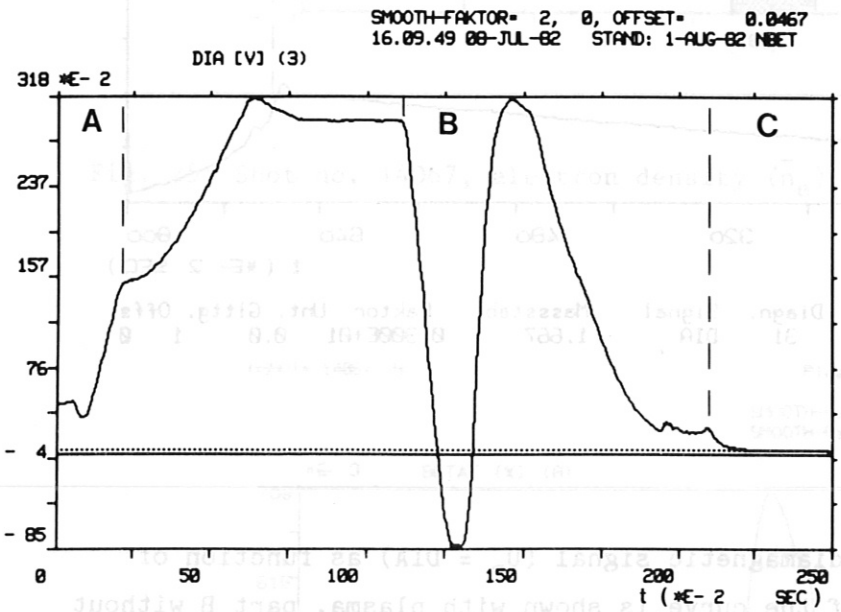

Fig. 29:

Shot no. 6357,
diamagnetic signal (U_D)
as function of time.

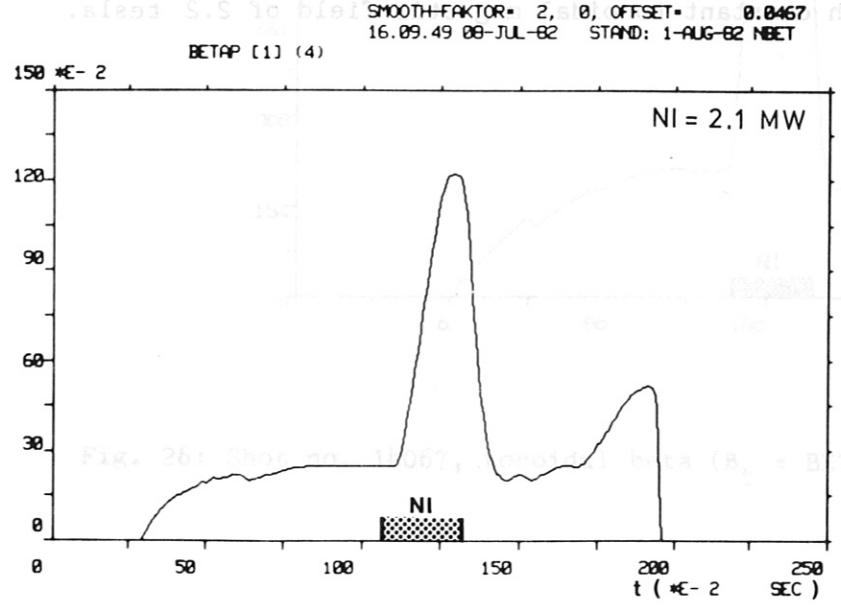

Fig. 30:

Shot no. 6357,
poloidal beta ($ß_{p\perp}$)
as function of time.

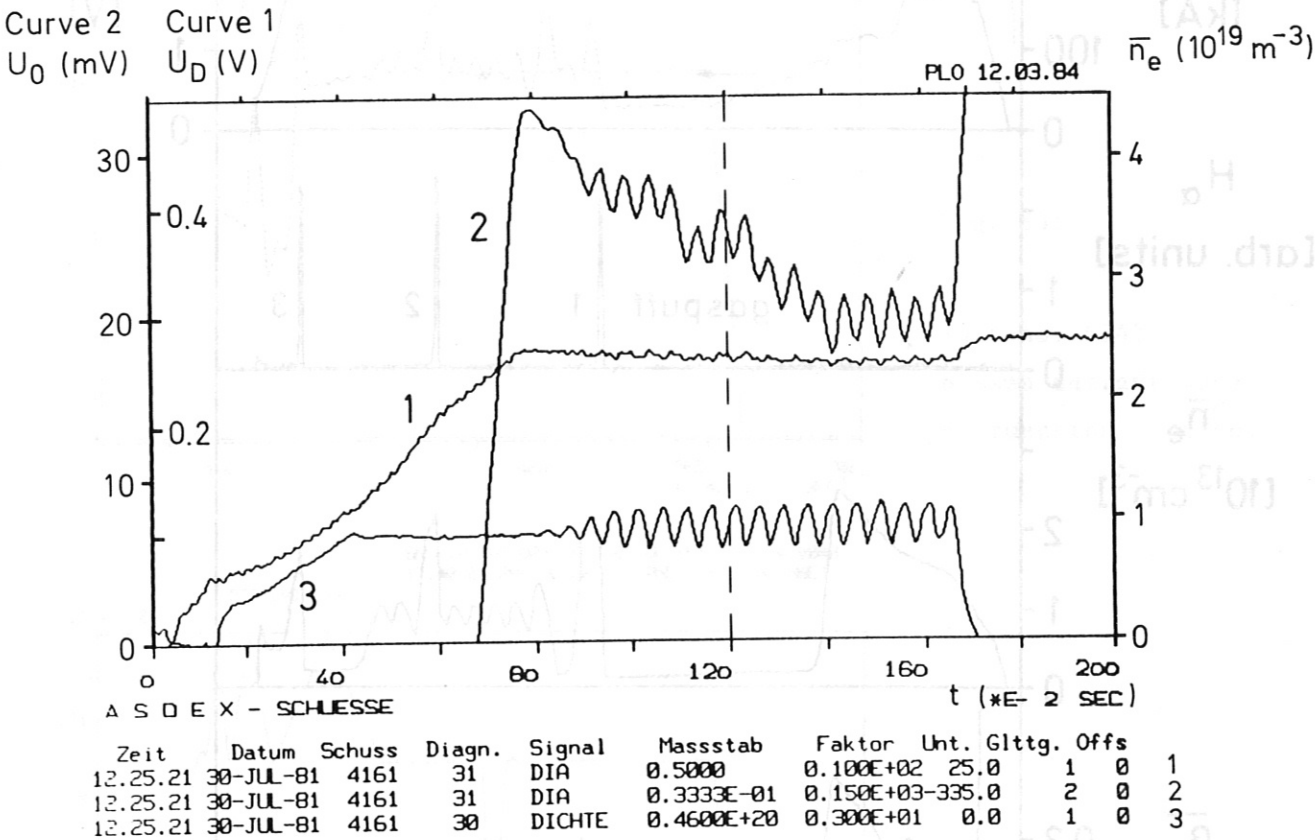

Zeit	Datum	Schuss	Diagn.	Signal	Massstab	Faktor	Unt.	Gttg.	Offs	
12.25.21	30-JUL-81	4161	31	DIA	0.5000	0.100E+02	25.0	1	0	1
12.25.21	30-JUL-81	4161	31	DIA	0.3333E-01	0.150E+03	-335.0	2	0	2
12.25.21	30-JUL-81	4161	30	DICHTE	0.4600E+20	0.300E+01	0.0	1	0	3

Fig. 31: Shot no. 4161, electron density $\bar{n}_e$ (curve 3), diamagnetic signal U_D (curve 1) with gain factor of 10 and diamagnetic signal U_D (curve 2) versus time with a gain factor of 150. Time constant for the active integrator of U_D was τ = 33 msec.

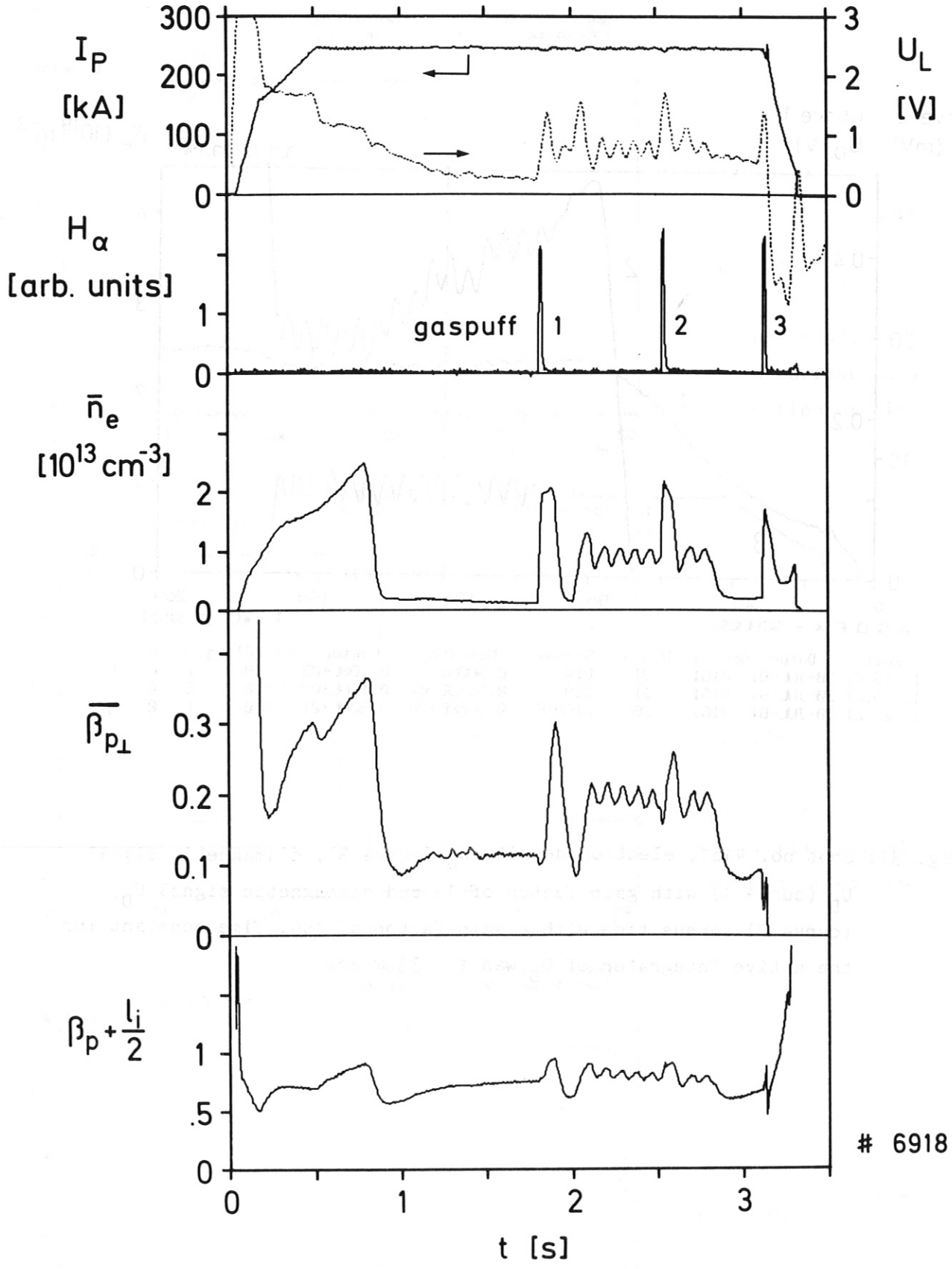

Fig. 32: Various plasma parameters for a slide-away discharge (shot no. 6918) with three fast gas puffs (indicated by increased H_α-intensity.

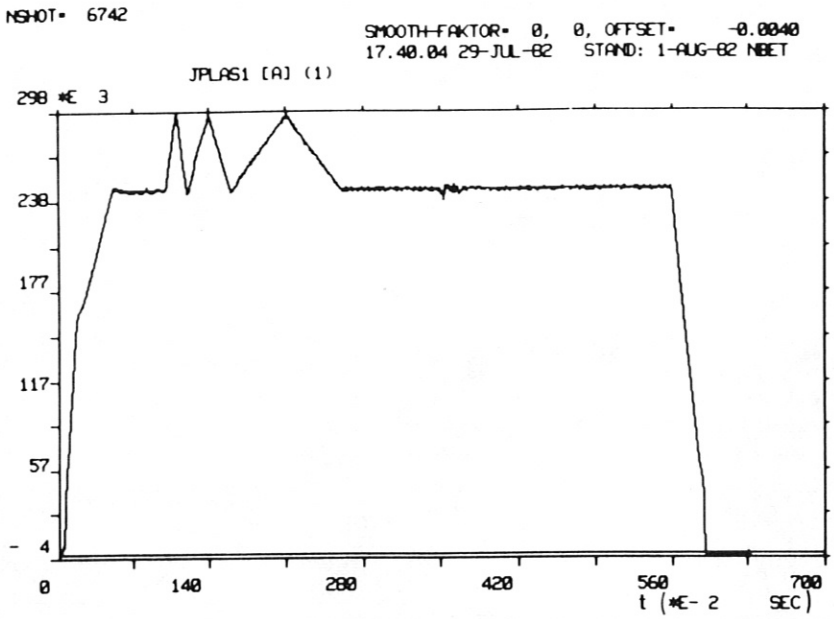

Fig. 33:

Shot no. 6742,
plasma current (J_p)
as function of time.

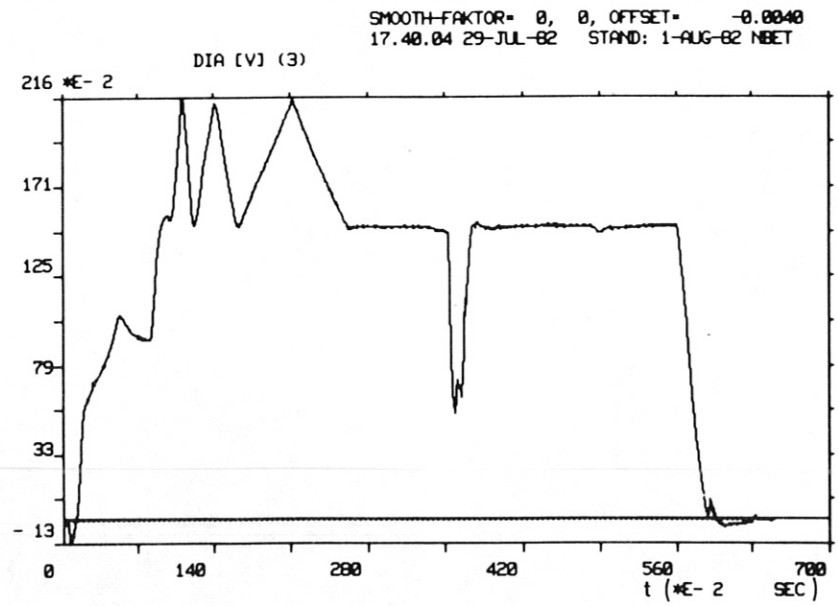

Fig. 34:

Shot no. 6742,
diamgnetic signal (U_D)
as function of time.

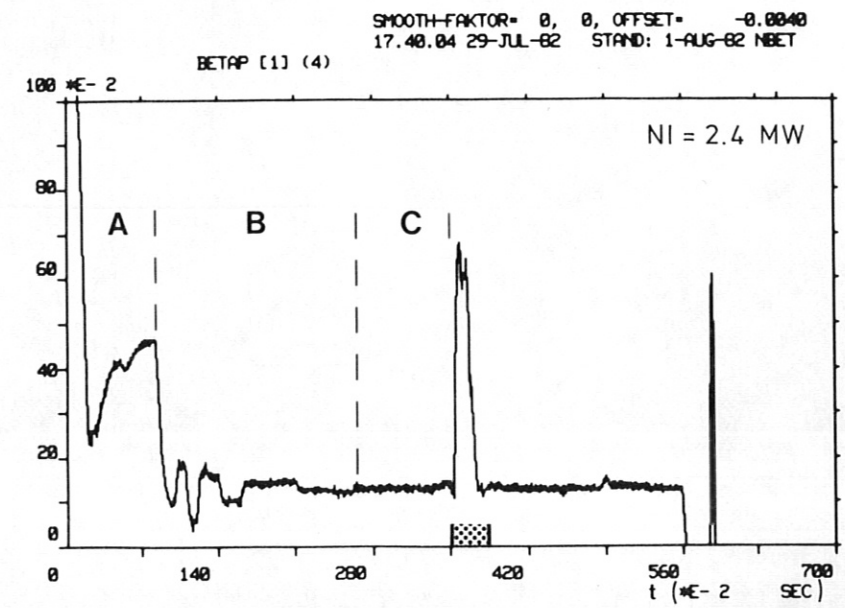

Fig. 35:

Shot no. 6742,
poloidal beta ($ß_{p\perp}$)
as function of time